Tissue Correlates of Hypoxic/ischemic MR Imaging Changes: Differences between Neonatal and Young Rats

By

Min Qiao

A thesis

Submitted to the Faculty of Graduate Studies

in Partial Fulfillment of the Requirements

for the Degree of

MASTER OF SCIENCE

Department of Physiology

University of Manitoba

Winnipeg, Manitoba

THE UNIVERSITY OF MANITOBA

FACULTY OF GRADUATE STUDIES

*****

COPYRIGHT PERMISSION PAGE

Tissue Correlates of Hypoxic/Ischemic MR Imaging Changes:

Differences between Neonatal and Young Rats

BY

Min Qiao

A Thesis/Practicum submitted to the Faculty of Graduate Studies of The University of Manitoba in partial fulfillment of the requirements of the degree of

Master of Science

ABSTRACT

Diffusion-weighted (DW) and T_2-weighted (TW) magnetic resonance (MR) imaging techniques have successfully detected ischemic changes in a variety of stroke models. Recently, it has been reported that there are age-dependent differences in the MR imaging changes observed during and after an episode of cerebral hypoxia/ischemia. The biophysical mechanisms for MR changes remain undefined. We hypothesized that the age-dependent MR changes in hypoxia/ischemia (occlusion of the right carotid artery plus exposure to 8% oxygen) were due to the developmental differences in hypoxia/ischemia-induced changes in brain water, cell volume control and/or cell death. Thus, we investigated the correlation between MR changes and alterations in brain water, Na^+-K^+-ATPase activity, cytochrome oxidase activity and cell death at various times following the start of hypoxia/ischemia until 24 hours of reperfusion in neonatal (1 week old) and young (4 week old) rats. We found that MR changes correlated well with many of the tissue alterations in neonatal brain but only partially in young brain: (i) Hypoxia/ischemia-induced changes in T_2 relaxation times correlated well with temporal alterations in brain water in 1 week old rats but early elevations in brain water in 4 week old rats could not be detected by TW imaging; (ii) Hypoxia/ischemia-induced DW changes corresponded to temporal alterations in brain Na^+-K^+-ATPase in 1 week old rats; however persistent decreases in Na^+-K^+-ATPase occurring immediately after hypoxia/ischemia in 4 week old rats were not reflected in the DW images; (iii) Hyperintensity areas in DW and TW images occurred 30 - 45 minutes after the onset of hypoxia/ischemia in 1 week old rats whereas in 4 week old rats hyperintensity changes in DW images appeared 10 - 15 minutes after the onset of hypoxia/ischemia and the T_2

changes occurred at 24 hours of reperfusion. The onset of T_2 changes corresponded to the disturbance in water dynamics in 1 week old brain and the presence of cell death in 4 week old brain; (iv) Areas of hyperintensity in DW and TW images 24 hours after hypoxia/ischemia corresponded to areas of infarction in both age groups; (v) The area with a decrease in cytochrome oxidase reaction product at 24 hours of reperfusion correlated well to the area of hyperintensity in MR images and the area of infarction morphologically. The results suggest that hypoxia/ischemia-induced T_2 and DW changes reflect alterations in water content and Na^+-K^+-ATPase in neonatal brain, respectively. However, there is only a partial correspondence in young brain suggesting that there might be other factors contributing to the developmental differences in the visibility of hypoxic/ischemic MR changes. The early T_2 changes in neonatal brain likely reflect the disturbance in water dynamics whereas the late T_2 changes 24 hours after cerebral hypoxia/ischemia in both neonatal and young brain likely reflect cell death.

ACKNOWLEDGEMENTS

I am very grateful to my supervisor, Dr. Ursula Tuor, for her knowledge and her commitment to guiding me through my studies. I would like to thank the members of my Advisory Committee, Dr. Larry Jordan and Dr. Marc Del Bigio for their helpful advice. Thanks also to Dr. Kris Malisza and Mr. Tadeusz Foniok for their assistance in MR imaging and Mrs. Saro Bascaramurty for her technical assistance in the animal experiments. Finally, special thanks to my husband for his consistent understanding and support throughout my studies.

LIST OF FIGURES

LIST OF TABLE

TABLE OF CONTENTS

INTRODUCTION

Continuous delivery of oxygenated blood and energy substrates to the brain is required to maintain cell viability. Although the human brain only constitutes about 2% of the body mass, it is responsible for 20% of the total oxygen consumption with the brain reserves of energy substrates being modest compared to its high rate of oxygen consumption (Lutz, 1994). Thus, an interruption of delivery in oxygen (hypoxia) and blood flow (ischemia) to the brain results in brain damage. Stroke with its resulting mortality and morbidity or poor prognosis has major adverse effects on the patients, their families and society. Early accurate diagnosis of the pathological changes in stroke and understanding of its cellular effects would potentially help in planning therapy and improving neurological function.

Over the past few years, the application of nuclear magnetic resonance (MR) techniques in medical biology has developed rapidly and been demonstrated to be of great benefit for clinical diagnosis (Gonzalez *et al.*, 1999; Sofka *et al.*, 1999). Unlike other traditional diagnostic devices, such as X-ray, CT, PET or angiography, which are invasive or potentially harmful to patients and clinical staff, MR techniques can provide a non-invasive detection of acute or chronic pathological changes in biological tissues. Diffusion-weighted (DW) and T_2-weighted (TW) MR imaging techniques which obtain image contrast from the diffusion of water and the magnetic relaxation of protons have been used to detect pathological changes in a variety of stoke models (Gill *et al.*, 1995; Loubinoux *et al.*, 1997; Tuor *et al.*, 1998). However, the biophysical mechanisms responsible for the abnormal MR signal in ischemia and its histological correlates remain poorly defined.

There is recent evidence to indicate that early MR changes during and following hypoxia/ischemia may differ in neonatal and young rats (Ning *et al.*, 1999; Tuor *et al.*, 1998). Whether these MR changes reflect different hypoxia/ischemia-induced changes in brain water or tissue damage is not clear. Surprisingly, few studies correlate MR changes with alterations in brain water or other tissue changes, particularly at the early stage of hypoxia/ischemia. Thus, in the present study, we investigated the correlation of MR changes with tissue alterations in brain water and Na^+-K^+-ATPase at a variety of times following the onset of cerebral hypoxia/ischemia in neonatal and young rats. 1 and 4 week old rats were used in this study because the maturity of rat brain at these stages corresponds to that in the human newborn and young children, respectively (Brody *et al.*, 1987; Tuor *et al.*, 1996). Changes in mitochondrial function in hypoxia/ischemia were assessed by histochemical examination for cytochrome oxidase activity. Pathological changes were investigated with hemotoxylin & eosin (H & E) staining or Annexin V labeling.

BACKGROUND INFORMATION

1) T_2 relaxation in T_2-weighted imaging

Matter is composed of subatomic particles (protons, neutrons and electrons). Their spinning around the nucleus like a cone-shaped top (called a precession) is associated with the generation of a magnetic field. When protons are placed in an external magnetic field, the spins precess with the central axis parallel to the direction of the external force (Chakeres and Schmalbrock, 1992). Each type of nuclear spin precesses at a specific frequency based on the static magnetic field (B_0). If an external radio frequency pulse (RF) is applied perpendicular to the direction of B_0 with a frequency equal to the natural system (also called the resonance frequency), the orientation of the spins will flip from the equilibrium (B_0) to the transverse plane perpendicular to the axis of B_0. This process is called excitation of protons (Sigal, 1988). Initially, all the spins precess at the same frequency of the RF pulse. The net magnetization, which is the total vector sum of many individual spins, is large when the spins all have the same phase organization. When the RF pulse is terminated, the transverse magnetization can be recorded as a signal by the RF coil. Following a RF pulse, the signal rapidly decays owing to the loss of phase organization of the individual spins in relation to one another and gradually return to equilibrium (Fig. 1). This process of the loss of phase organization is called T_2 relaxation and this is associated with time constant of the T_2 relaxation (Sigal, 1988). To measure the T_2 relaxation time, a series of spin-echo images are acquired and the time of repetition (TR) between images is kept constant. The maximum signal for each image decreases as the

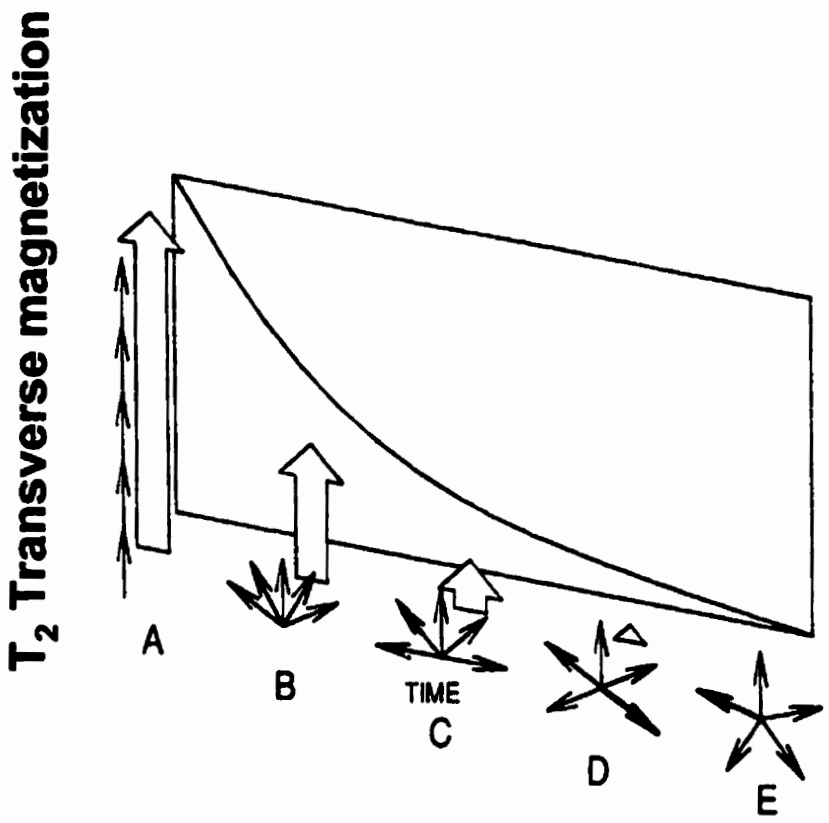

Fig.1. Sketch showing T_2 relaxation of protons. Following a 90^0 radio frequency pulse, the signal rapidly decays versus time due to a loss of phase organization of individual spins.

time of echo (TE) lengthens owing to the T_2 relaxation. A plot of signal intensity versus TE provides an exponential decay curve from which to calculate the T_2 relaxation times.

Most tissues of the body are predominately composed of water. Thus, the signal originating from detectable protons in magnetic resonance (MR) images comes from water molecules in the tissue. The common measurements made from TW images are signal intensity and T_2 relaxation time. The corresponding biological phenomena monitored are the content of water and its dynamic interactions in a complex biological environment (Mathur de Vre, 1984). Several factors affect the T_2 signal acquired in TW images. In general, the more protons in the tissue, the more net transverse magnetization and the higher TW intensity. In addition to the proton density, the T_2 signal in the body is also dependent on intrinsic microscopic environment. Water in tissue can either bind to macromolecules (bound water) or exist freely in tissue (free water) where the two have different T_2 relaxation times. An understanding of the effects by which the chemical matrix of the tissue alters the relaxation times of its constituent water is very important in the overall understanding of TW images (Cameron *et al.*, 1984; Fullerton *et al.*, 1982; Inch *et al.*, 1974; Mathur de Vre, 1984). For example, it has been shown that the T_2 relaxation of water at the same concentration in a solution of cellulose is much different from that in a solution of gelatin (Chakeres and Schmalbrock, 1992). Indeed, the magnitude of T_2 in biological tissue is affected by the microscopic alternating fields of the nuclear spins. If two spin dipoles are in close proximity, the two magnetic spins will affect each other and will result in a fluctuation or inhomogeneity of the local magnetic field. Pure water has a longer T_2 because of the homogeneous local magnetic field, whereas water in a biological tissue has a shorter T_2 because of local field fluctuations

originating from the interaction of water molecules with macromolecules. Mathur de Vre (1984) suggested that the following water-macromolecule interactions might contribute to the measured T_2 in biological tissues:

(i) Restricted motion involving translation and rotation of water molecules.

(ii) Partial orientation of water molecules with respect to the macromolecular chains.

(iii) Multiple frequencies of motion and distribution of correlation times (Tc), where Tc is the average time between molecular collisions and varies between 10^{-6} and 10^{-9} s in the hydration layer (bound water), and has a value of 10^{-12} s for free water.

(iv) Anisotropic diffusion and enhanced proton transfer along the hydration layer.

(v) Anisotropic rotation and decoupling of translational and rotational motion of water molecules due to macromolecular-water interactions.

(vi) Differential interaction potential along the charged macromolecular chains.

Other factors influencing T_2 relaxation are paramagnetic or superparamagnetic substances (Brasch, 1983; Hahn *et al.*, 1987; Stark *et al.*, 1988; Thulborn *et al.*, 1982) and field inhomogeneity. Paramagnetic substances are molecules and atoms with chemically unpaired electrons. They are associated with a large magnetic moment, approximately 700 times as powerful as the nuclear magnetic moment. It is known that deoxygenated hemoglobin is paramagnetic and induces a signal loss in T_2-weighted images (Thulborn *et al.*, 1982). Superparamagnetic substances consist of very small crystals of ferric or ferromagnetic compounds and have a powerful magnetic property (Hahn *et al.*, 1987).

Both paramagnetic and superparamagnetic substances influence the intrinsic relaxation properties of water by producing local magnetic field inhomogeneity.

2) Water diffusion in diffusion-weighted (DW) imaging

The signal obtained in DW images depends on diffusion behavior of water. Molecules in a fluid move in a microscopic random pattern, a so-called Brownian motion or self-diffusion. The property of diffusion is represented by a diffusion coefficient, which is proportional to the mean square of the distance covered per time. The measurement of water diffusion using MR techniques was established more than two decades ago (Stejskal and Tanner, 1965). In a spin-echo sequence without gradients, the signal drops exponentially with echo time because of the intrinsic T_2 relaxation. When strong gradients are turned on, the diffusing spins acquire different phases, not only because of the intrinsic T_2 relaxation but also because of the random motion in the presence of gradients. Therefore, the net transverse magnetization reduces more rapidly and the observed signal decays even faster. The signal decay is faster if the magnetic field gradients are stronger and if the spins have a higher diffusion coefficient. Elimination or reduction of T_2 effects can be achieved either by using very large gradient factors or by the acquisition of two data sets, one with and one without a diffusion gradient. When using very large gradient factors, diffusion effects dominate over T_2 effects and the result is a DW image in which regions of high water diffusion have a low signal intensity (Huppi and Barnes, 1997; Stejskal and Tanner, 1965; van Bruggen *et al.*, 1994).

In biological systems, diffusion of water is impeded by the presence of cell membranes, organelles and macromolecules resulting in a reduced apparent diffusion

coefficient (ADC) with less signal attenuation than freely diffusible water. Contrast in the DW images is influenced by local ADC and thus depends on the microenvironment of tissue and the physiological status, including cell membrane permeability, exchanges between free and bound water and tortuosity of the diffusion path (van Bruggen *et al.*, 1994). Water diffusion in tissue may appear anisotropic when the translational movement of water is more restricted or hindered in one direction than others. Thus, white matter tracts parallel to the diffusion-sensitizing gradients appear dark, whereas those in the perpendicular orientation are bright. This phenomenon has been called "directional anisotropy" in DW images (Hossmann and Hoehn Berlage, 1995).

3) Hypoxic/ischemic MR imaging changes

Numerous studies have demonstrated that hyperintense areas in DW images or regions with a decreased ADC occur as soon as a few minutes after the onset of ischemia (Kohno *et al.*, 1995; Mintorovitch *et al.*, 1991; Moseley *et al.*, 1990). In contrast to DW changes, there are no detectable T_2 changes until 3 - 24 hours post ischemia. T_2 changes at 24 - 48 hours correspond well to the distribution of infarction (Allegrini and Sauer, 1992; Barone *et al.*, 1991; Tuor *et al.*, 1998). Based on the temporal evolution of ischemic MR changes, changes in DW and TW images have been assumed to reflect cellular and vasogenic edema, respectively (Kimelberg, 1995; Loubinoux *et al.*, 1997). However, the biophysical mechanisms responsible for the abnormal MR signal in ischemia remain poorly understood.

A decrease in ADC following ischemia corresponds to severe reductions in blood flow, reductions in ATP, and decreased extracellular space measured by electrical

impedance in the tissue (Hoehn Berlage *et al.*, 1995; Hossmann *et al.*, 1994; van Lookeren Campagne *et al.*, 1994). In severe cerebral hypoxia/hypoxia, a loss of oxygen and blood supply leads to a quick drop of energy metabolites, such as ATP and phosphocreatine. If the reduced level of ATP is not enough to maintain the function of Na^+-K^+-ATPase, extracellular Na^+ moves into the intracellular space along its concentration gradient resulting in the influx of water osmotically from the extracellular space (Hansen and Olsen, 1980). Limitation of water diffusion due to increased tortuosity of the diffusion path through the shrunken extracellular space results in a slower attenuation of signal loss in DW images and this is reflected as a hyperintensity or a decrease of the ADC in DW images (van Lookeren Campagne *et al.*, 1994; Verheul *et al.*, 1994). Although the shrinkage of extracellular space occurring in cellular edema has been thought to be the major factor contributing to the decreased ADC in ischemic brain, there is little evidence to support this assumption due to the technical difficulties in the direct measurement of the extracellular compartment. Na^+-K^+-ATPase is an important enzyme involved in cell volume control and it therefore might serve as a sensitive marker for changes in extracellular space. There is one study showing a mild correlation in the trend of changes in DW images and in Na^+-K^+-ATPase activity in an adult stroke model of middle cerebral artery occlusion (MCAO) (Mintorovitch *et al.*, 1994). Whether changes in Na^+-K^+-ATPase correlate with the changes in DW images in cerebral hypoxia/ischemia is unknown.

As mentioned above, an increase in the number of water protons is associated with an increase in the T_2 times (Chakeres and Schmalbrock, 1992). Thus, TW changes in ischemia have been assumed to reflect changes in water content of the tissue

(Loubinoux *et al.*, 1997; Mintorovitch *et al.*, 1991; Ning *et al.*, 1999; Tuor *et al.*, 1998). However, few studies correlate the T_2 changes with alterations in brain water content. There are reports that an increase in T_2 corresponds to the increase in brain water content 24 – 72 hours after focal cerebral ischemia in a MCAO stroke model (Boisvert *et al.*, 1990; Naruse *et al.*, 1991). To the best of our knowledge, there has been no report that follows the spatial and temporal changes in T_2 and brain water from the start of ischemia or hypoxia/ischemia until 24 hours of reperfusion during which time energy status and water dynamics go through distinctive alterations (Lorek *et al.*, 1994; Mujsce *et al.*, 1990; Slivka *et al.*, 1995). Furthermore, recent studies reported that there were differences in the onset and resolution of T_2 changes between neonatal and young rat brain during and following cerebral hypoxia/ischemia (Ning *et al.*, 1999; Tuor *et al.*, 1998). In those studies, the correlation between T_2 changes and alterations in brain water content was not studied.

4) Cellular edema

Fluid in the central nervous system is distributed in the intracellular and extracellular spaces of brain parenchyma, the cerebrospinal fluid (CSF), and the vascular compartment. Homeostasis of fluid in the body is required for normal cellular function. Any increase of brain water (brain edema) (Go, 1997) might raise intracranial pressure or cause herniation in the brain. Brain edema is classified into cellular edema (also called cytotoxic edema) and vasogenic edema based on its pathogenesis (Go, 1997; Klatzo, 1967; Kimelberg, 1995). A disturbance of homeostasis in ions and water takes place in both types of edema.

Cellular edema occurs in intoxication, deep hypothermia, and the early stage of anoxia or ischemia. This type of edema is defined as cell swelling resulting from intracellular accumulation of water and Na^+ (Go, 1997). There are at least three different mechanisms responsible for the control of cell volume. First, Na^+-K^+-ATPase exchanges 3 intracellular Na^+ ions for 2 extracellular K^+ ions with the hydrolysis of 1 molecule of ATP for each full pumping cycle. Interference with Na^+-K^+-ATPase function by a reduction in energy availability leads to an influx of Na^+ from the extracellular space and an obligate influx of water into the cell. Second, the membrane ion channels for Na^+, K^+, or Cl^- also make a contribution to maintaining ion balance across the membrane. Third, the activation of cotransport or countertransport (antiporter) systems (Cala *et al.*, 1988) are involved in the regulation of pH and cell volume (Eveloff and Warnock, 1987). For example, the Na^+/H^+ antiporter is activated in the presence of acidosis to extrude the intracellular H^+ in exchange for an influx of Na^+ with an inflow of water.

5) Vasogenic edema

Vasogenic brain edema is considered to be a consequence of blood brain barrier (BBB) breakdown resulting in leakage of plasma constituents, such as protein, water and electrolytes into parenchyma of the brain (Klatzo *et al.*, 1967). The disruption of BBB occurs in focal cerebral lesions, such as cerebral contusions, brain trauma, tumors, inflammatory lesions and the later stage of cerebral ischemia. Morphologically, the BBB consists of cerebral capillary endothelium, together with tight junctions occluding the clefts between endothelial cells (Go, 1997). Protein leakage from the systemic circulation indicates an increased permeability of the BBB via either separation of tight junctions or

increased pinocytosis (vesicular transport) (Brightman *et al.*, 1973; Go, 1997). Opening of the BBB often takes place 3 - 6 hours after the onset of ischemia (Balayer *et al.*, 1996; Menzies *et al.*, 1993). Clearance of fluid occurs by reabsorption into capillaries, drainage into the CSF, uptake and degradation by glial elements, or drainage to the lymph nodes (Bradbury *et al.*, 1981; Klatzo *et al.*, 1980).

6) Age dependent differences in extracellular space and brain water

Water content in the newborn brain is high and declines with age (Agrawal *et al.*, 1968). This is attributed to the postnatal maturation in neurons and glial cell processes. Extracellular space in brain also decreases with age. Lehmenkuheler *et al.* (1993) reported that extracellular space in the cerebral cortex was largest in newborn rats and a dramatic reduction in extracellular space occurred between postnatal day 10 - 21. There was no further decrease in volume fraction between postnatal day 21 and adults (90 -120 days old). Thus, the relatively large extracellular space in neonatal brain would allow a dilution of the substances released from cells and the vascular compartment, such as water, ions, excitatory neurotransmitters and metabolic substrates related to the pathological insult. This is supported by the finding that the latency for ischemia-induced shrinkage of the extracellular space is longer in 4 – 6 day old rat brain compared to 21 – 23 day old rat brain (Vorisek and Sykova, 1997).

RATIONALE

There is evidence that hypoxia/ischemia-induced changes in DW and TW images are different in neonatal and young brain (Ning *et al.*, 1999; Tuor *et al.*, 1998). The reason for these age differences in MR imaging is unknown. Changes in DW and TW images in biological tissues are considered to be due to the alterations in the extracellular space and water content, respectively (van Lookeren Campagne *et al.*, 1994). Thus, it is possible that age-dependent MR changes are due to age differences in brain water dynamics and extracellular space (Vorisek and Sykova, 1997). Furthermore, since Na^+-K^+-ATPase plays an important role in cell volume control, it is also possible that changes in Na^+-K^+-ATPase activity reflect alterations in extracellular space. Finally, some of the differences in MR imaging may be due to age-dependent differences in cell injury or cell detected. Histologically, cell injury can be assessed with the histochemical analysis for cytochrome oxidase, H&E staining or Annexin V labeling. Cytochrome oxidase, the final enzyme complex in the respiratory chain on the inner mitochondria membrane, is involved in oxidative phosphorylation and ATP generation in mitochondria (Balaban, 1990). Punctate chromatin, pyknosis or eosinophilic cells on H & E stained sections indicate cell death. The translocation of phosphatidylserine from the inner plasma membrane to the external surface of cell membrane can be revealed by Annexin V labeling suggesting an early stage of apoptosis (Walton *et al.*, 1997).

HYPOTHESIS AND OBJECTIVES

We hypothesize that age-dependent differences in hypoxic/ischemic DW and TW images are due to a combination of different cellular changes in brain water, cell volume control, or mechanisms for cell injury during development. To test this hypothesis, we investigated:

1. Whether hypoxic/ischemic changes in DW images correspond to alterations in Na^+-K^+-ATPase.
2. Whether hypoxic/ischemic changes in T_2 correlate with alterations in brain water.
3. Whether hypoxic/ischemic changes in DW and TW images correspond to signs of cell injury or death as indicated by changes in cytochrome oxidase, Annexin V labeling and cell morphology.

MATERIALS AND METHODS

HYPOXIA/ISCHEMIA MODEL

Pregnant Wistar rats were obtained from Charles River Laboratories (Montreal, Canada) and gave birth approximately 1 week following their arrival. Following birth, each litter was culled to 8 - 10 pups and caged with the dam. All animals used in this study were treated in accordance with the guidelines provided by the Canadian Council on Animal Care and experiments were approved by the local Animal Care Committee. Animals were assigned to two age groups – 1 week and 4 week old rats. Cerebral hypoxia/ischemia was produced as previously described (Tuor *et al.*, 1998). The animals were anesthetized with isoflurane (3 - 4% for induction and 1.5 - 2.5% for maintenance) with a nose mask throughout the surgery. The neck was incised in the midline and the cervical field was infiltrated with 0.25% bupivicaine. The right common carotid artery was ligated with 2 pieces of 5-0 suture and severed between the suture knots. The incision site was closed with suture and skin glue (Nexoband, Veterinary Product Lab, Phoenix, AZ). Saline (0.1 ml/10g) was injected intraperitonially to compensate for the fluid losses during surgery. In the sham control group, the carotid artery was isolated but not ligated. Following surgery, the rats were returned to the cage to be with the mother for 1 - 2 hours of recovery from the anesthesia. Then, rats were subjected to hypoxia (humidified 8% O_2 + 92% N_2) for a duration of 2 hours (1 week old rats) or 30 minutes (4 week old rats). A similar extent of hypoxic/ischemic injury is produced with these durations of hypoxia in 1 week and 4 week old rats (Tuor *et al.*, 1996). Body temperature was maintained at 37.0 - 37.5^{0}C during hypoxia with water blanket on the top and/or bottom of the rat body, or by a temperature-controlled lamp.

EXPERIMENTAL DESIGN

In each age group (n=12/group), MR images were acquired 20 minutes before hypoxia (serving as baseline), throughout the whole period of hypoxia, at 1 hour or 24 hours of reperfusion using DW or TW imaging techniques (Fig. 2). After the last image, animals were killed with an overdose of pentobarbital (80 mg/kg). The brain was removed for the immediate determination of brain water and the rest of the brain was frozen for future histochemical and pathological examination (Fig. 2).

In several additional experiments (n = 26 in 1 week old rats; n = 21 in 4 week old rats), cerebral hypoxia/ischemia was produced without MR imaging. The rats were killed at the end of hypoxia, 1 hour or 24 hours of reperfusion. Animals with sham surgery but not ischemia/hypoxia served as controls (group assignment is shown in Fig. 2). Generally, the whole cerebrum was dissected into 3 parts (Fig. 2): the anterior cerebrum containing the striatum was removed for the measurement of brain water content using a dry/wet weighing method. The middle cerebrum was frozen in isopentane (- 45 ^{0}C) and stored at – 80 ^{0}C until it was used for histochemical or pathological examination for Na^{+}-K^{+}-ATPase, cytochrome oxidase, H & E staining or Annexin V labeling. The posterior cerebrum, a majority of cortex and some white matter and hippocampus was removed for the determination of tissue specific gravity, which is inversely proportional to the water content in the tissue.

A

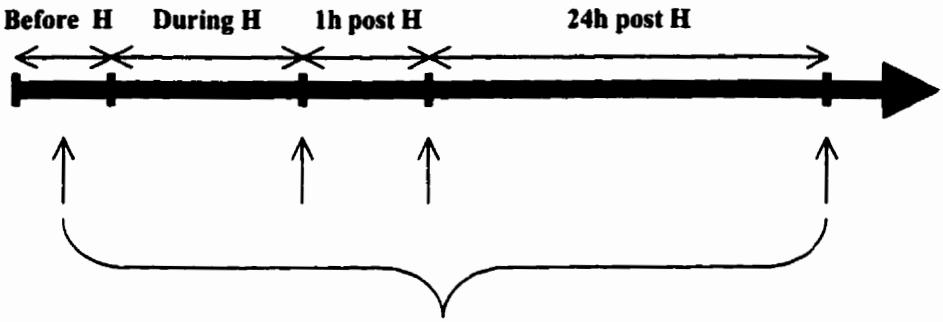

MR imaging, brain water measurement and histological studies.

B

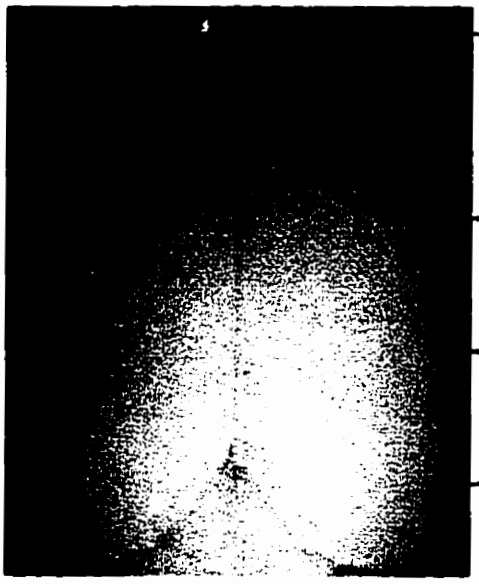

Anterior cerebrum - used for the determination of water content using dry/wet method

Middle cerebrum - frozen for the histological examinations: Na^+-K^+-ATPase, cytochrome oxidase, H & E or Annexin labeling

Posterior cerebrum - used for the determination of specific gravity using percoll method.

Fig. 2. Experimental protocol showing the times for the various measurements *(A)* and brain sampling sites for brain water measurement and histological studies *(B)*. *H: Hypoxia.*

MRI

MR experiments were performed in a 9.4T/21cm horizontal bore magnet (Magnex, UK) equipped with an MSLX Bruker console (Bruker, Germany). The animals were anesthetized with isoflurane (4% for induction, 0.25 -1.0% for maintenance) in 45% O_2 (1/3 O_2 + 2/3 air) and placed in a chamber designed to fit the bore of the magnet. The animal was restrained by a foam-lined head holder (1 week old rats) or by ear pins and incisor bar (4 week old rats). While in the magnet, the ECG and respiration rate were monitored continuously in 1 week old and 4 week old rats, respectively. A water blanket with circulating water was placed on the top and /or the bottom of the rat body to maintain the body temperature at 37.0 - 37.5^{0}C throughout hypoxia.

Rats were imaged immediately before hypoxia, during hypoxia, and at 1 hour or 24 hours of reperfusion. DW images and TW images were acquired with a quadrature coil tuned to 400.045 MHz. DW images were acquired with a Stejskal-Tanner spin-echo sequence (Stejskal and Tanner, 1965) (TR = 1200 ms, TE = 30 ms, 8 slices, 1 mm thick (1 week old rats) or 1.5 mm thick (4 week old rats), average of 4 (1 week old rats) or 2 (4 week old rats). Two diffusion-sensitive gradient pulses of 10 ms duration and 85 mT/m amplitude were separated by 25 ms, which resulted in b = 1062 s/mm^2. The diffusion gradient pulses were applied in the phase encoding (Y) direction. TW images were acquired with a multiecho sequence: TR = 1200 ms, TE = 21.6 ms, 6 echoes, 3 slices, 1mm thick (1 week old rats) or 1.5 mm thick (4 week old rats), average of 2. For both sequences, the field of view was 2 cm and the data matrix was 256 x 128.

MR images were analyzed with programs developed at the Institute for Biodiagnostics, National Research Council of Canada. The hyperintensity areas in TW or DW images were measured as a percentage of the entire brain slice at the coronal levels of striatum (anterior cerebrum), mid-thalamus (middle cerebrum) and posterior thalamus (posterior cerebrum) using the program *XVOL_MEASURE* or a computerized image analysis system (MCID, Imaging Research Inc., St. Catherines, Ontario, Canada). The T_2 relaxation times in the ipsilateral or contralatereal hemisphere were calculated from an analysis of the multiecho images with the program *EVIDENT*. For DW images, the mean relative intensity in the ipsilateral or contralatereal hemisphere was measured using the program *XVOL_MEASURE*.

BRAIN WATER DETERMINATION

Changes in brain water were determined with two methods. A dry/wet weighing method was used to determine the percentage of water content in the brain tissue and a percoll density gradient method was used to measure the specific gravity of brain tissue. To avoid water loss due to vaporization during the process of sampling, the decapitated rat head with the whole skull was quickly cooled in isopentane (- 35 ^{0}C) for 10 - 15 seconds. Then, the skull was removed and the brain was dissected into different parts for the measurement of water content or specific gravity. For the dry/wet method, 50 - 60 mg (1 week old rats) or 100 - 120 mg (4 week old rats) of brain from the left or right anterior hemisphere was removed and wrapped in a piece of preweighed aluminum foil. The wet tissue wrapped in foil was weighed followed by drying in an oven at 100 ^{0}C for 4 - 5 days

until the weight of the dry tissue was consistent. The percentage of water content was determined using the equation below:

$$\%\ Water\ content = (wet\ weight - dry\ weight) / wet\ weight \times 100$$

In general, a relatively large sample is preferred for water content measurements with the dry/wet weighing method. To overcome the possible inaccuracies of water content measurement obtained by the dry/wet method, another more accurate method for small samples - the specific gravity measurement was used to assess brain edema. To measure brain specific gravity, the linear density gradient was prepared with percoll (Pharmacia Biotech) and NaCl solution (Tengvar *et al.*, 1982). Stock isotonic percoll (SIP) was first prepared by diluting percoll with 1.5 M NaCl (v:v = 9:1). The SIP solutions were further diluted to "dense solution" with 0.15 M NaCl according to the recommendations provided by the manufacturer. An equal volume (50 ml) of dense solution and light solution (0.15 M NaCl) were mixed and pumped (5 ml/min) into a 100 ml cylinder where the final gradient was formed. After equilibration for 30 min, the depth of the linear gradient was calibrated with the standard beads (1.018-1.06 g/ml) (Pharmacia Biotech) and a regression equation of standard specific gravity versus the depth of the gradient was obtained. For the determination of specific gravity, 30 - 35 mg of brain tissue was removed and dropped into the percoll gradient. The sample sank slowly in the gradient and the standstill point of the floating sample was recorded. The specific gravity of tissue was calculated according to the calibration regression equation.

HISTOLOGICAL STUDIES

The block of middle cerebrum was cryosectioned at a thickness of 20 μm. After air drying at room temperature for 30 min, some of these sections were used for cytochrome oxidase staining, whereas others were immersion fixed in 10% formalin for Na^+-K^+-ATPase examination or fixed in acetone for H&E staining or Annexin V labeling.

Na^+-K^+-ATPase

Histochemical detection for Na^+-K^+-ATPase was examined with a one-step lead citrate method (Mayahara and Ogawa, 1988). The formalin-fixed sections were washed in dH_2O for 2 x 5 min, then incubated with the enzyme reaction medium (250 mM glycine-KOH buffer, 4 mM lead citrate, 10 mM p-nitrophenyl phosphate (NPP), 25 % dimethyl sulfoxide (DMSO), 2.5 mM levamisole) at 37^0C for 2 hours (1 week old brain) or 35 minutes (4 week old brain). This was followed by reaction with 1% ammonium sulfide for 30 seconds. A pilot study with a variety of incubation periods was performed to choose the best incubation times for 1 week and 4 week old brain. Several different control experiments were conducted:

a) To demonstrate K^+ dependency of Na^+-K^+-ATPase activity, K^+ was removed from the original incubation medium. This was achieved by substituting glycine-NaOH buffer for glycine-KOH and lead citrate-NaOH for lead citrate-KOH.

b) To demonstrate inhibition of the reaction, 10 mM ouabain was added to the incubation medium.

c) To compare localization of nonspecific alkaline phosphatase activity with that of Na^+-K^+-ATPase, levamisole, an inhibitor of alkaline phosphatase, was removed from the incubation medium.

d) A negative control was conducted by replacing the reaction substrate of NPP with dH_2O.

e) A positive control was performed by staining a section of kidney.

MCID system was used to measure the relative intensity for Na^+-K^+-ATPase reaction product. Five optical density readings were made in the ipsilateral and contralateral hemispheres at the level of mid thalamus. The area with a reduction in Na^+-K^+-ATPase reaction product was measured as a percentage of the entire brain section with the MCID system.

Cytochrome oxidase

The cytochrome oxidase assay was done using a previously published method (Nelson and Silverstein, 1994; Tuor *et al.*, 1994). Briefly, fresh sections were incubated in the dark in a reaction medium consisting of 0.5 mg/ml diaminobenzidine, 250 μg/ml cytochrome *c*, 4% sucrose in 0.1M PBS at 37^0C for 2 hours (1 week old brain) or for 30 minutes (4 week old brain). A pilot study with a variety of incubation periods was performed to choose the best incubation time for 1 week and 4 week old brain. A negative control experiment was also conducted in the absence of the substrate for cytochrome *c*.

The MCID system was used to measure the relative intensity for cytochrome oxidase reaction product. Five optical density readings were made in the ipsilateral and

contralateral hemispheres at the level of mid thalamus. The area with a reduction in cytochrome oxidase reaction product was measured as a percentage of the entire brain section with the MCID system.

H & E staining and Annexin V labeling

Cell injury or death was assessed with standard H & E staining and Annexin V labeling using light microscopy. A frozen section at the level of middle cerebrum from each animal was stained with H & E and then examined for signs of edema, pyknosis, punctate chromatin, and infarction. Infarction was quantified by measuring the areas with a reduction or loss in H & E staining on brain sections. For Annexin V labeling, frozen brain sections were washed in PBS for 3 x 5min and then incubated with biotinylated Annexin V (1:100, Cedarlane Lab, Ontario, Canada) in the dark at room temperature overnight (Walton *et al.*, 1997). The binding of Annexin V was revealed with an ABC kit (Cedarlane Lab) and diaminobenzidine. To demonstrate the presence of condensed chromatin after Annexin V labeling, a nuclear dye consisting of propidium iodide (1 μg/ml) was added on the section. For the negative control, 1x binding buffer was added instead of Annexin V. The cells with double labeling of Annexin V and propidium iodide were considered apoptotic cells.

STATISTICAL ANALYSIS

All the data were presented as mean ± SD. Areas of MR hyperintensity, reduction in enzyme reaction product and infarction were presented as a percentage of the entire brain slice. The intensity of DW images and enzyme reaction product, T_2 relaxation times, specific gravity and water content were displayed as relative ratios measured in ipsilateral/contralateral hemisphere. Even though the absolute values for T_2 times and brain water were available, they were presented as relative ratios in this study because even a 1 - 2 day variability in gestation and birth date in this model could greatly affect the absolute values and the standard deviation of the means. Furthermore, we noticed that brain water content in the contralateral hemisphere in bigger rats was lower than that in smaller rats even though they are at the same age. A Bonferroni-test or a Dunn's test was used for comparing mean hyperintensity areas in both DW and TW images, or mean ratios of T_2 times, DW intensity, intensity for Na^+-K^+-ATPase and cytochrome oxidase reaction product at different times. Differences were considered significant at $P < 0.05$. Least square regression analysis was used to analyze the correlation of: T_2 changes with alterations in water content, DW changes with alterations in Na^+-K^+-ATPase reaction product, MR hyperintensity area with the distribution of infarction or area of decreased cytochrome oxidase, or area of decreased cytochrome oxidase reaction product with area of infarction.

RESULTS

MRI

The patterns of changes in DW images were similar in both age groups during and after an episode of hypoxia/ischemia. However, the onset of hyperintensity in DW images occurred earlier in 4 week old rats than 1 week old rats. T_2 changes during and immediately after the termination of hypoxia were different in 1 week and 4 week old rats.

1) One week old rats

Prior to hypoxia, there was no difference in brightness of the ipsilateral and contralateral hemispheres in DW and TW images. As early as 30 - 45 minutes after the start of hypoxia, both TW and DW images appeared hyperintense in the ipsilateral hemisphere within the territory of the right common carotid artery. With continuing hypoxia, DW changes in the ipsilateral hemisphere spread to the contralateral cortex in 3/5 rats. At the end of 2 hours hypoxia, hyperintensity in both DW and TW images became significant with areas of hyperintensity in the striatum, cortex, hippocampus, thalamus and hypothalamus (Fig. 3). At this time, the mean areas of hyperintensity in the DW images were 58% ± 0.30, 54% ± 0.22, 49% ± 0.22 at the levels of anterior, middle and posterior cerebrums, respectively (Fig. 4A). Compared to the extensive changes in DW images during hypoxia, the areas of hyperintensity in TW images were much smaller (14 % - 26 %) at the corresponding brain levels (Fig. 5A). In addition, the distribution of TW changes was generally restricted to the ipsilateral hemisphere except for one animal, which showed a small area of hyperintensity in the contralateral hemisphere adjacent to

the dorsal midline. Quantitatively, the ratios of T_2 relaxation time in the ipsilateral/contralateral hemisphere were greater than the values pre-hypoxia by 7% - 9% (Fig. 5B). The intensity ratios in DW images had an average of 43% - 70% increase compared to the values pre-hypoxia (Fig. 4B).

Upon termination of hypoxia, both TW and DW hyperintensity changes diminished rapidly. At 1 hour of reperfusion, DW and TW images were similar to those acquired before hypoxia except for a small area of hyperintensity remaining in DW images in the ipsilateral cortex and thalamus at the level of middle cerebrum (Fig. 3 and Fig. 4A). The T_2 ratio at middle cerebrum recovered substantially but still remained significantly higher than that before hypoxia (Fig. 5B).

At 24 hours of reperfusion, a hyperintensity in both DW and TW images re-appeared in the ipsilateral cortex, striatum, hippocampus, thalamus and hypothalamus (Fig. 3). At this time, the areas of hyperintensity in DW images were less than those during hypoxia (Fig. 4A and B). However, the T_2 ratio was higher and the areas of hyperintensity in TW images exceeded those during hypoxia.

2) 4 week old rats

Prior to hypoxia, there was no difference in brightness within the ipsilateral and contralateral hemispheres in DW and TW images. During hypoxia, there were ipsilateral increases in intensity in DW images but not TW images (Fig. 6). The first changes in DW images occurred about 10 – 15 minutes after the onset of hypoxia and the areas of hyperintensity reached 22% - 25% of the whole brain level at the end of 30-minute of hypoxia (Fig. 7A, B). Within 1 hour of reperfusion, areas of DW hyperintensity in the

ipsilateral hemisphere disappeared and the TW images were similar to those obtained pre-hypoxia (Fig. 6; Fig. 7A; Fig. 8A). Intensity and T_2 ratios in DW and TW images were similar to controls (Fig. 7B and Fig. 8B). Indeed, the whole brain at this time appeared "normal". After 24 hours of reperfusion, hyperintensity in DW images returned with overall smaller areas in the ipsilateral hemisphere compared to the values obtained during hypoxia (Fig. 7A). Hyperintensity areas in TW images also appeared in the ipsilateral striatum and cortex, particularly in the anterior cerebrum (Fig. 8A, B). In slices within the middle or posterior cerebrum, only the hippocampus and small areas of the cortex appeared hyperintense. Furthermore, the most significant change in T_2 times was in the ipsilateral anterior striatum (90 ± 4 ms vs 80 ± 2 ms in the contralateral striatum).

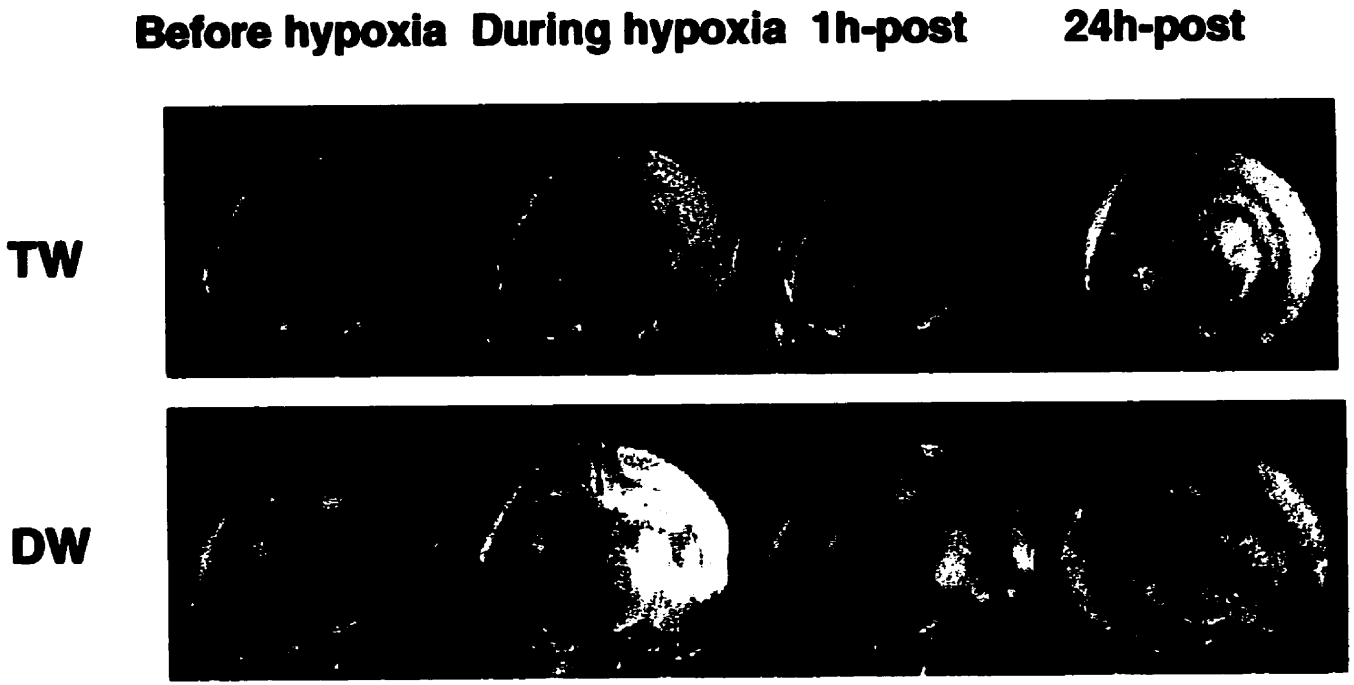

Fig. 3. Hypoxic/ischemic changes in T_2-weighted (TW) and diffusion-weighted (DW) images in 1 week old rats. Images were acquired before hypoxia, during hypoxia and at 1 or 24 hours of reperfusion. Hypoxic/ischemic hemisphere appears bright (right) on the MR images.

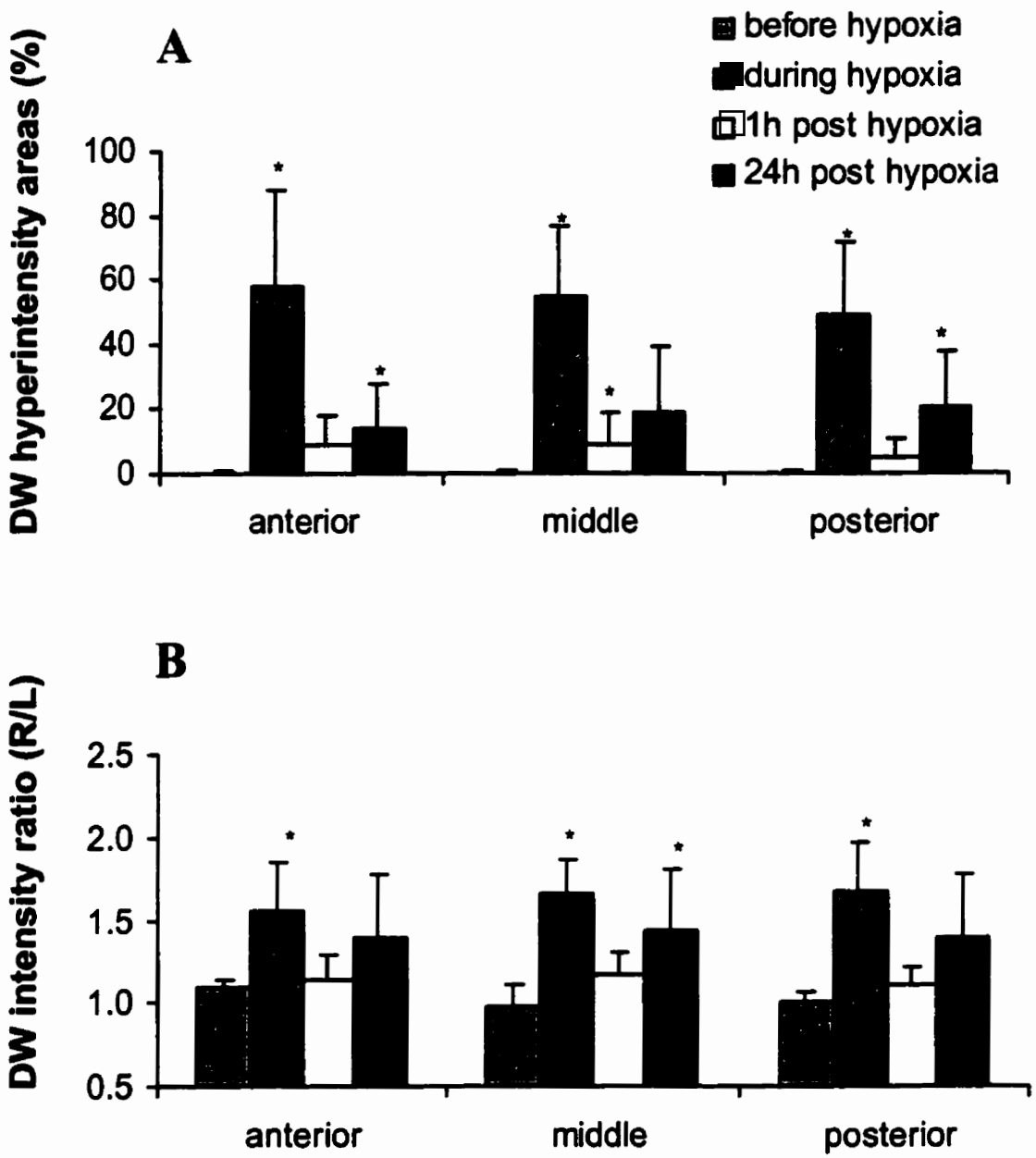

Fig. 4. Hypoxic/ischemic hyperintensity changes in diffusion-weighted (DW) image in 1 week old rats. (A) showing the mean hyperintensity areas presented as a percentage of the entire brain slice, and (B) showing the mean ratio of relative intensity in ipsilateral/contralateral hemisphere (R/L) at the brain levels of anterior, middle or posterior cerebrum. * $P < 0.05$ vs. before hypoxia.

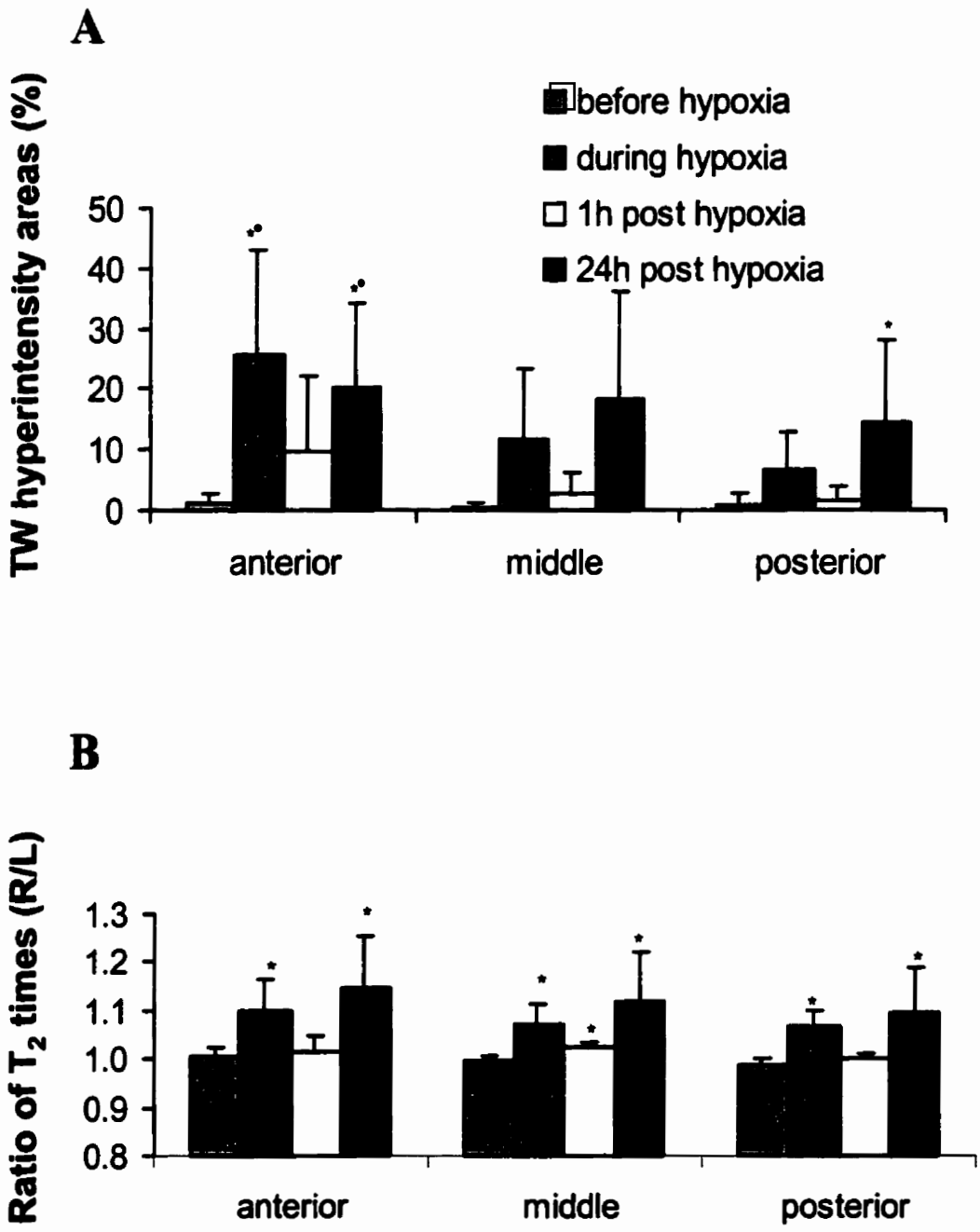

Fig. 5. Hypoxic/ischemic hyperintensity changes in T_2-weighted (TW) image in 1 week old rats. (A) showing the mean hyperintensity areas presented as a percentage of the entire brain slice, and (B) showing the mean ratio of relative intensity in the ipsilateral/contralateral hemisphere (R/L) at the brain levels of anterior, middle or posterior cerebrum. * $P < 0.05$ vs. before hypoxia.

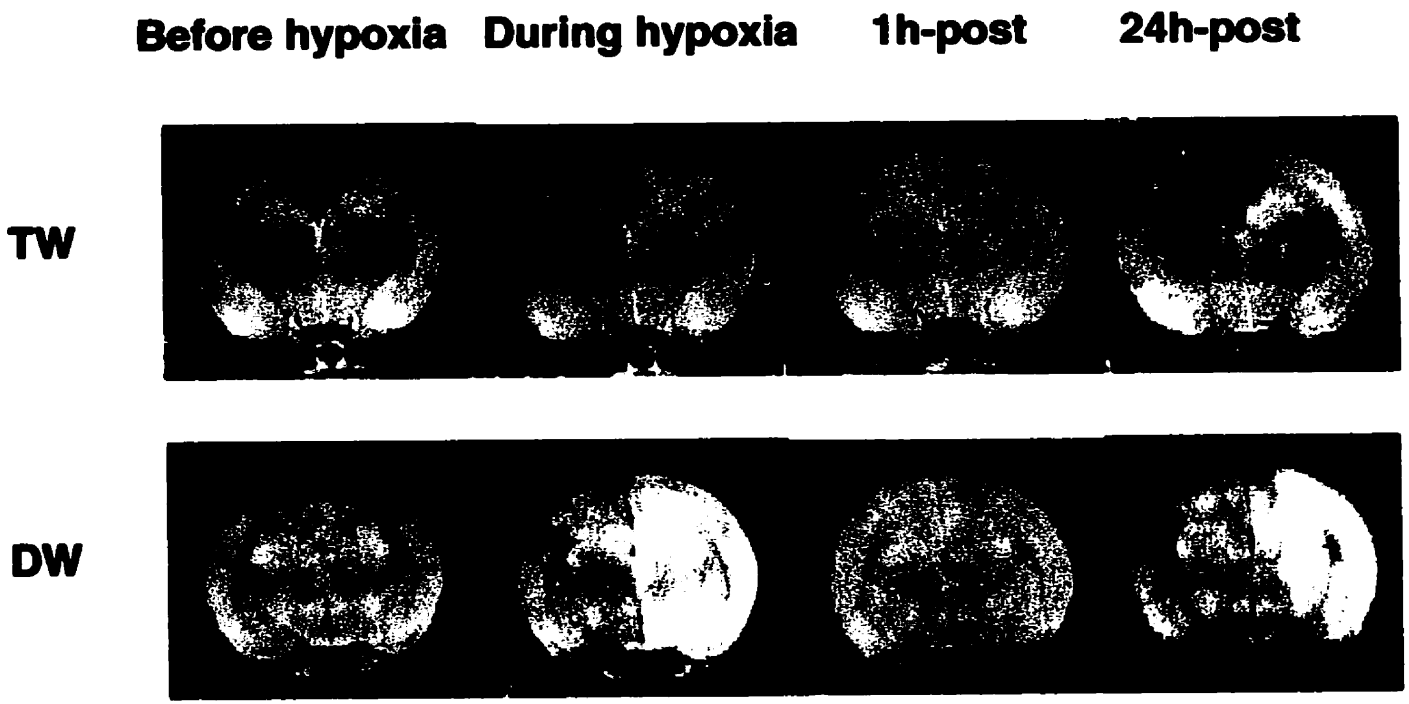

Fig. 6. Hypoxic/ischemic changes in T_2-weighted (TW) and diffusion-weighted (DW) images in 4 week old rats. Images were acquired before hypoxia, during hypoxia and at 1 or 24 hours of reperfusion. Hypoxic/ischemic hemisphere (right) appears bright on the MR images.

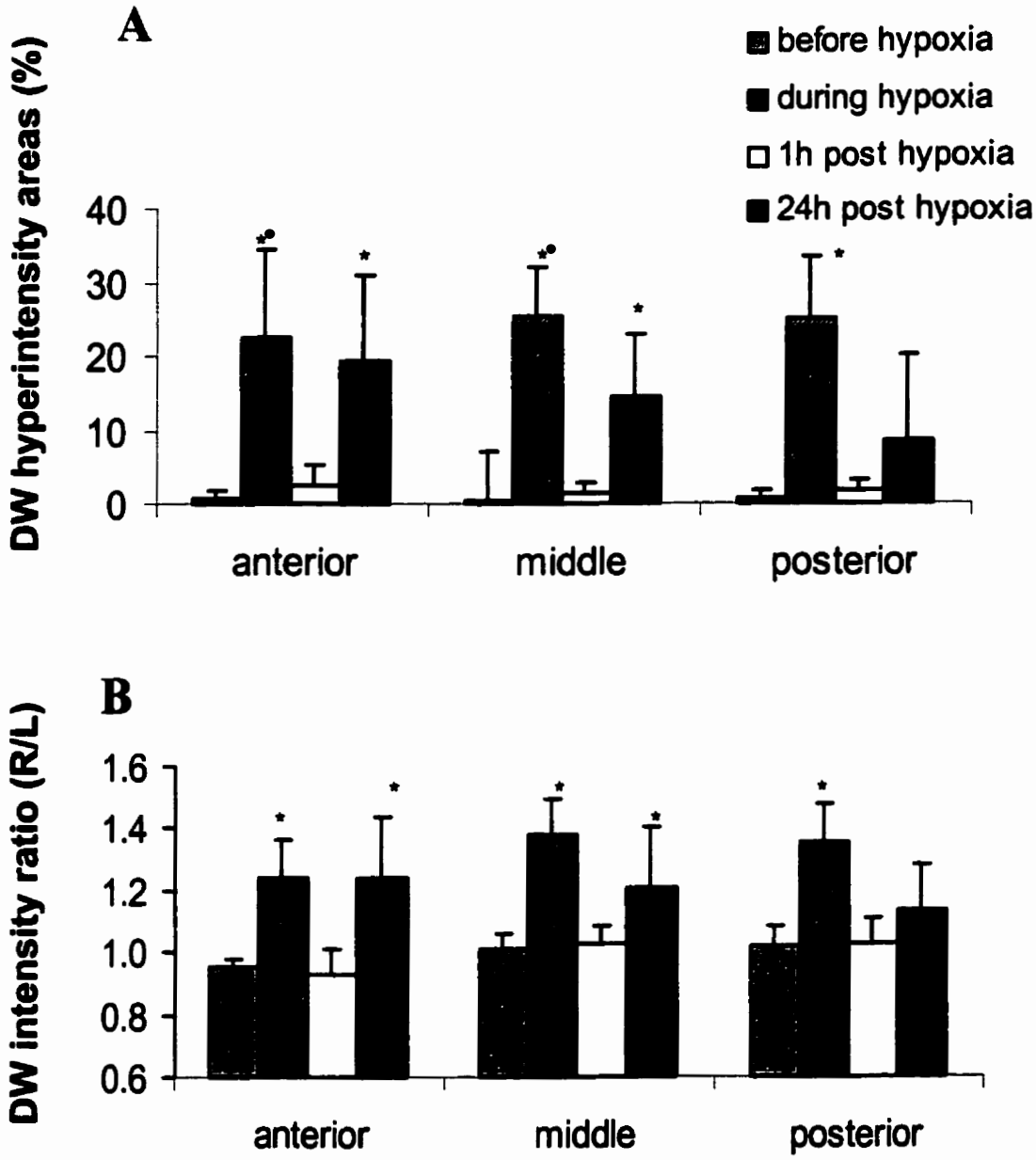

Fig. 7. Hypoxic/ischemic hyperintensity changes in diffusion-weighted (DW) image in 4 week old rats. (A) showing the mean hyperintensity areas presented as a percentage of the entire brain slice, and (B) showing the mean ratio of relative intensity in the ipsilateral/contralateral hemisphere (R/L) at the brain levels of anterior, middle or posterior cerebrum. * $P < 0.05$ vs. before hypoxia.

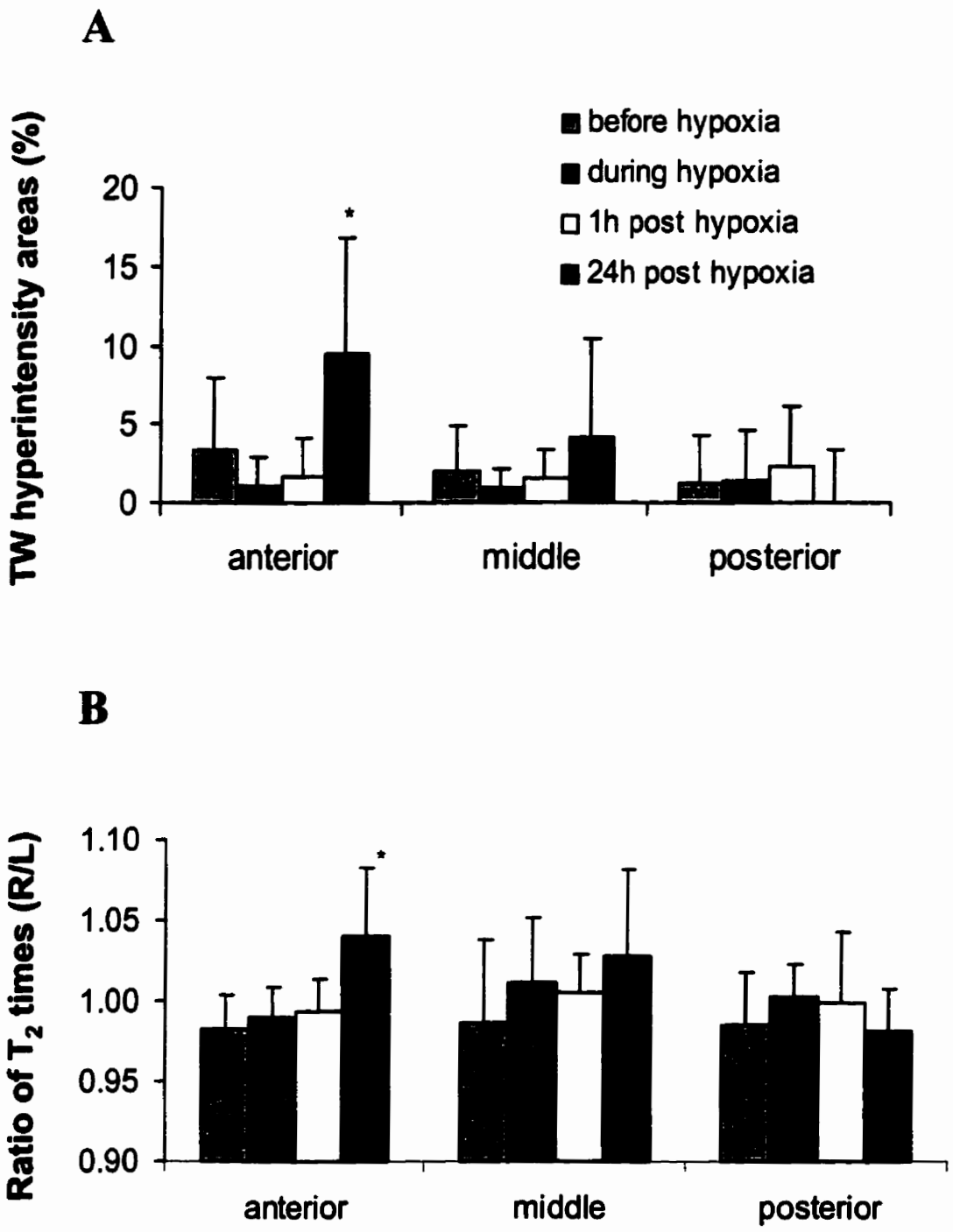

Fig. 8. Hypoxic/ischemic hyperintensity changes in T_2-weighted (TW) image in 4 week old rats. (A) showing the mean hyperintensity areas presented as a percentage of the entire brain slice, and (B) showing the mean ratio of relative intensity in the ipsilateral/contralateral hemisphere (R/L) at the brain levels of anterior, middle or posterior cerebrum. * $P < 0.05$ vs. before hypoxia.

BRAIN WATER

In the control groups, there was a decrease in brain water with postnatal development between 1 week to 4 weeks (88.50% ± 0.001, 81.13% ± 0.003, respectively). No difference in brain water content was found between the contralateral and ipsilateral hemispheres in any group of sham controls, irrespective of age. The changes in brain water over the time course of hypoxia/ischemia in neonatal brain differed from those in young brain. Brain water in 1 week old brain increased during hypoxia followed by a marked recovery immediately after the termination of hypoxia whereas there was no recovery in 4 week old animals.

1) 1 week old rats

Ipsilateral to the carotid occlusion, water content ratio in the anterior cerebrum increased by 0.95% during hypoxia ($P < 0.05$) and exhibited a trend towards recovery within 1 hour of reperfusion (Fig. 9A). Although the water content ratio after 1 hour of reperfusion remained slightly higher than that in control group, the difference was not statistically significant. A secondary increase in brain water occurred at 24 hours of reperfusion with water content ratio being 1.92% higher than that in the control group. There were corresponding changes in specific gravity, which are inversely related to the brain water content. Specific gravity ratio in the posterior cerebrum showed a decrease during hypoxia followed by a partial recovery at 1 hour of reperfusion and a secondary decrease at 24 hours of reperfusion (Fig. 9B).

2) 4 week old rats

During hypoxia, water content ratio increased by 1% ($P < 0.05$) (Fig. 10A) and specific gravity decreased (Fig. 10B). The absolute water content in the hemisphere ipsilateral to the carotid occlusion was lower compared to that in 1 week old rats during hypoxia (82.23% ± 0.003 vs 88.80% ± 0.005). Unlike the changes in neonatal brains, there was no trend towards recovery in water content or specific gravity after 1 hour of reperfusion (Fig. 10A, B). At 24 hours of reperfusion, water content ratio in the anterior cerebrum remained 1.39% higher than control levels although there appeared to be a partial recovery of specific gravity in the posterior cerebrum (Fig. 10A, B).

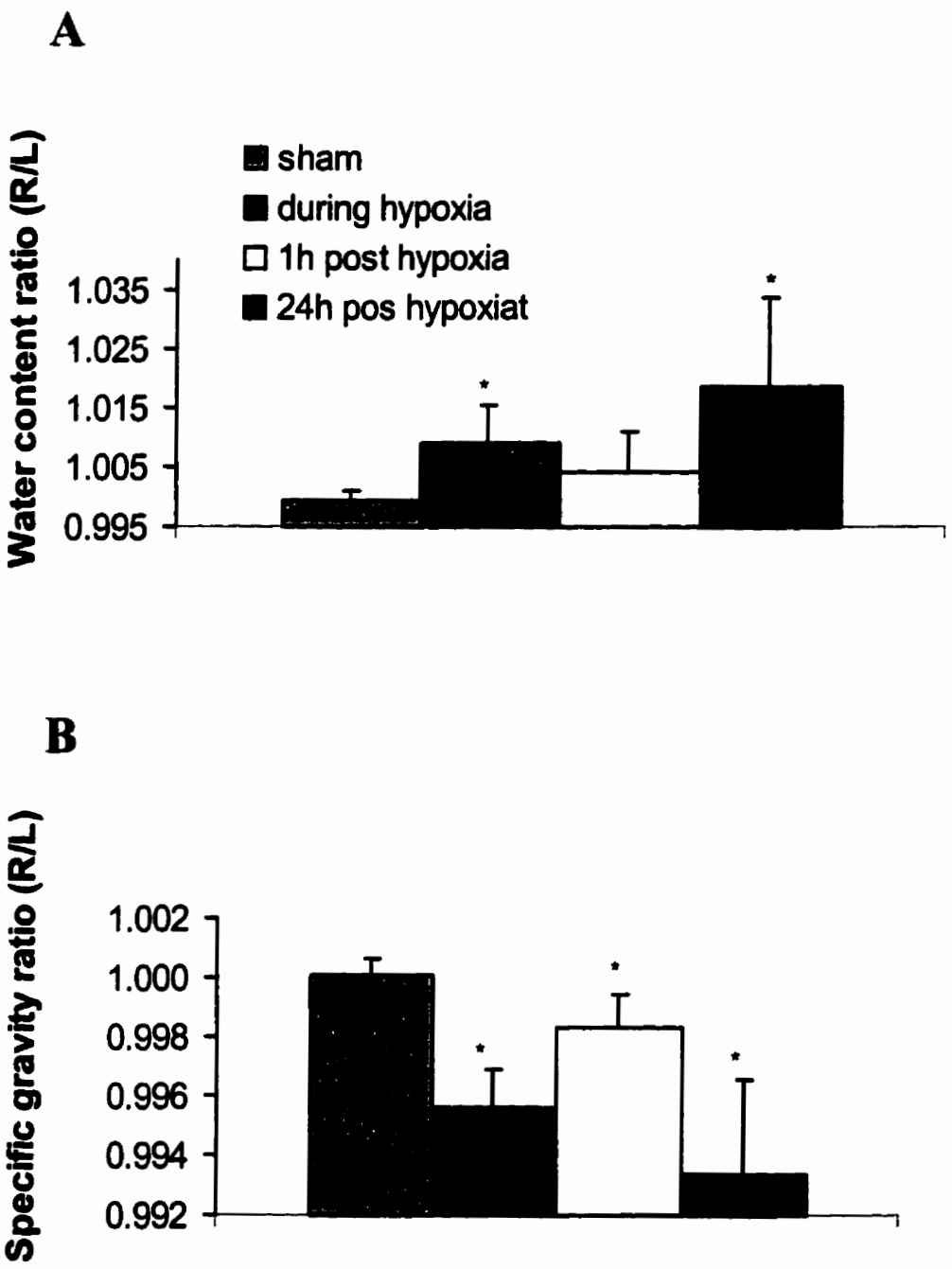

Fig. 9. Hypoxic/ischemic changes in brain water in 1 week old rats. Brain water is measured as water content (A) in the anterior cerebrum or specific gravity (B) in the posterior cerebrum. Data are presented as the mean ratio of values in the ipsilateral/contralateral hemisphere (R/L). * $P < 0.05$ vs. sham control.

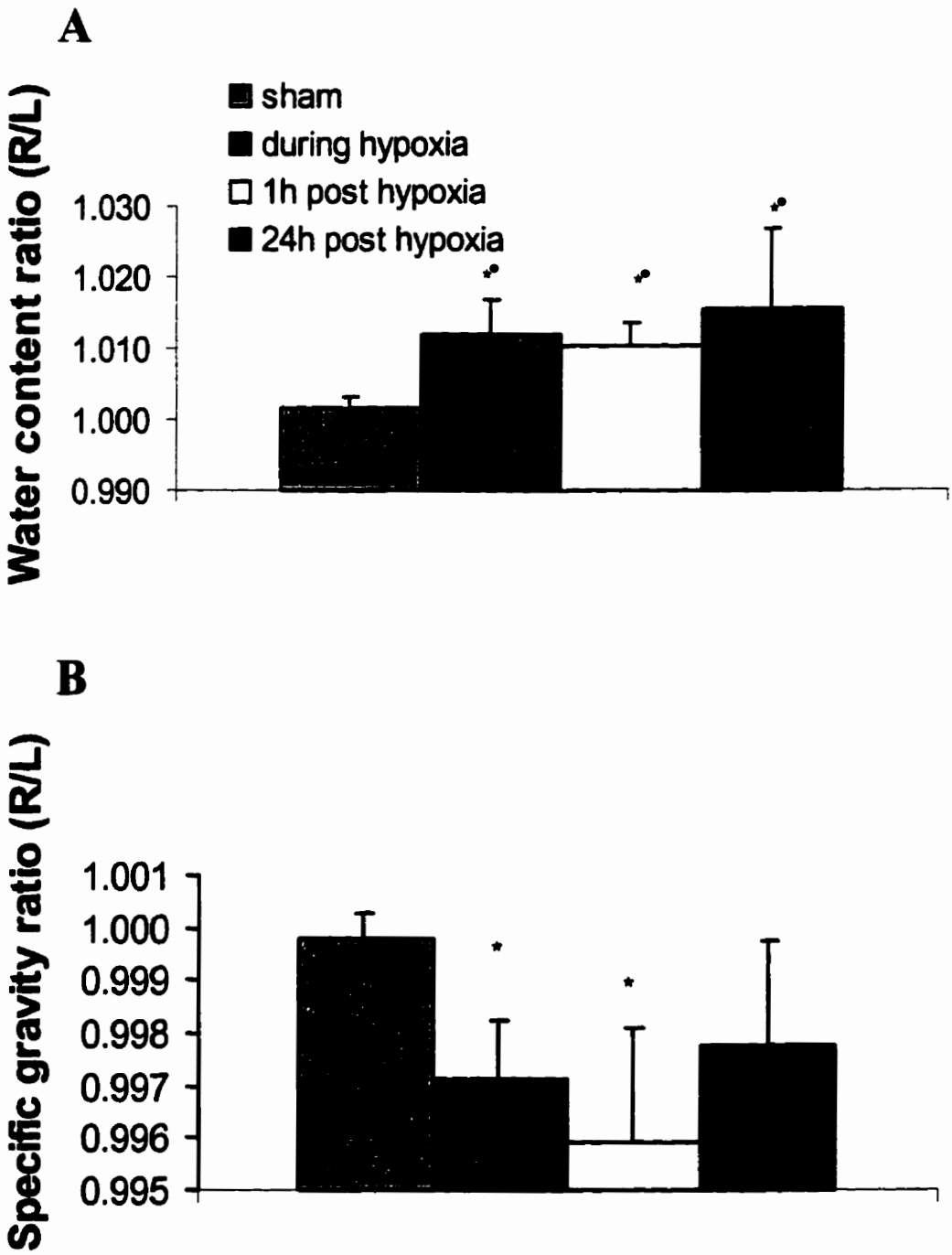

Fig. 10. Hypoxic/ischemic changes in brain water in 4 week old rats. Brain water is measured as water content (A) in the anterior cerebrum or specific gravity (B) in the posterior cerebrum. Data are presented as the mean ratio of values in the ipsilateral/contralateral hemisphere (R/L). * $P < 0.05$ vs. sham control.

Na^+-K^+-ATPase

In the control animals, there were age dependent differences in Na^+-K^+-ATPase activity or density. The intensity ratio of enzyme reaction product for Na^+-K^+-ATPase was lower in 1 week old brain despite using a 4-fold longer incubation time than that required in 4 week old brain. As a consequence, the background intensity was greater in 1 week old brains. For the positive control experiments, intensity for Na^+-K^+-ATPase reaction product in kidney was very strong because of its higher activity of Na^+-K^+-ATPase than brain. The reaction was blocked or inhibited by the elimination of K^+ or the addition of ouabain in the reaction medium. Non-specific alkaline phosphatase activity was inhibited well in the presence of levamisole.

In 1 week old rats, a slight decrease in Na^+-K^+-ATPase reaction product was found in the ipsilateral region of CA_3 during hypoxia. Within 1 hour of reperfusion, the histochemical detection for Na^+-K^+-ATPase was similar to that in the control group. At 24 hours of reperfusion, a decrease in Na^+-K^+-ATPase reaction product became evident in the regions of the dentate gyrus, CA_1, CA_2, and CA_3 sectors (Fig. 11).

In 4 week old rats, the intensity for Na^+-K^+-ATPase reaction product during hypoxia showed an apparent decrease in almost the entire hemisphere ipsilateral to the occlusion. There was no recovery within 1 hour of reperfusion (Fig. 12). 24 hours after the termination of hypoxia, Na^+-K^+-ATPase showed some recovery in all regions in the ipsilateral hemisphere but a reduction in Na^+-K^+-ATPase reaction remained in the dentate gyrus, CA_1, CA_2, CA_3, cortex and thalamus.

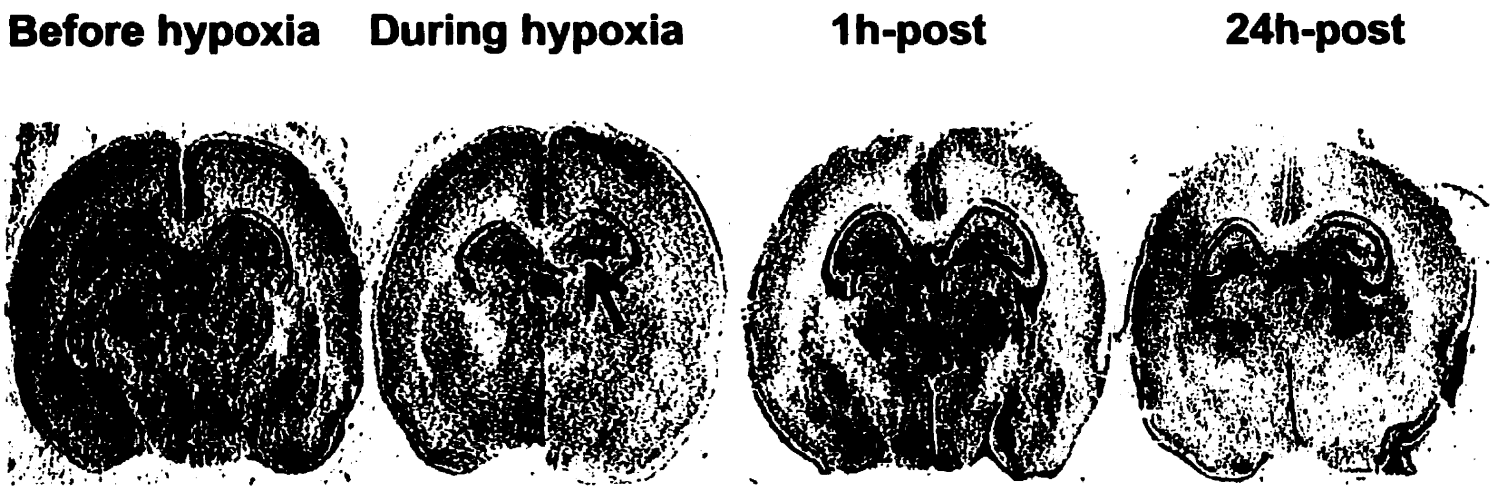

Fig. 11. Hypoxic/ischemic changes in Na^+-K^+-ATPase in 1 week old rats. A decrease in Na^+-K^+-ATPase reaction product occurs in the hippocampus (arrow) ipsilateral to the carotid occlusion during hypoxia ($P < 0.05$). At 1 hour of reperfusion, there is no difference in Na^+-K^+-ATPase between the ipsilateral and contralateral hemispheres. A decrease in Na^+-K^+-ATPase reaction product in the hippocampus becomes evident at 24 hours of reperfusion.

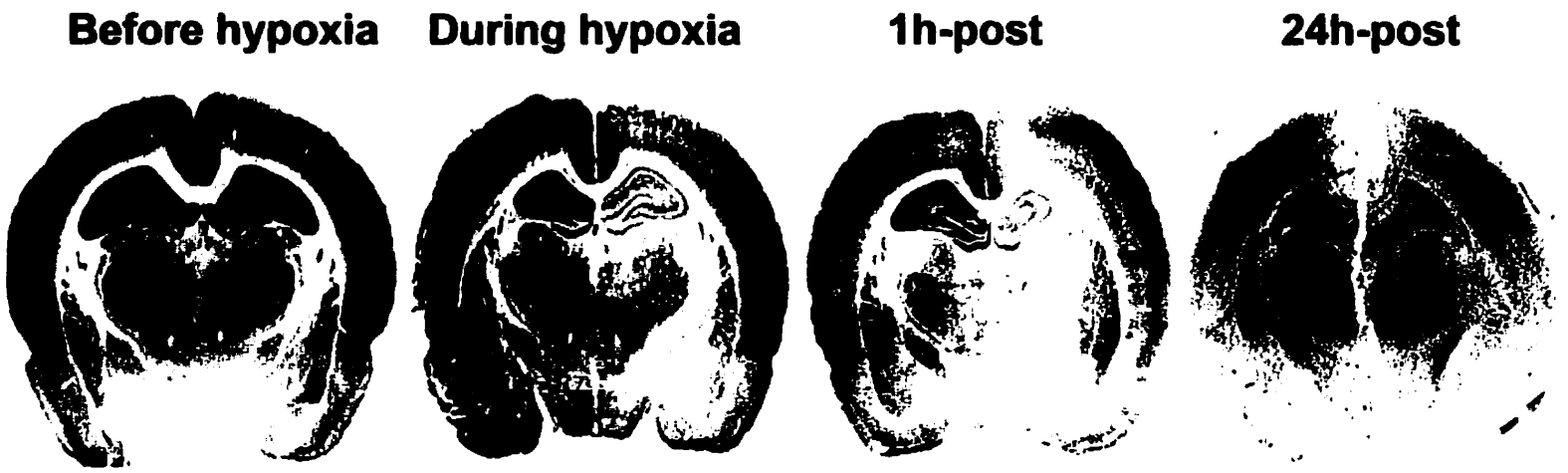

Fig. 12. Hypoxic/ischemic changes in Na^+-K^+-ATPase in 4 week old rats. A decreases in Na^+-K^+-ATPase reaction product occurs in the hemisphere (right) ipsilateral to the carotid occlusion during hypoxia and at 1 hour of reperfusion. At 24 hours of reperfusion, decreases in Na^+-K^+-ATPase reaction product remain in the hippocampus, cortex and thalamus ipsilateral to the occlusion.

CYTOCHROME OXIDASE

During hypoxia, there was a modest decrease in the reaction product for cytochrome oxidase in the dentate gyrus ipsilateral to the occlusion in 1 week old brain. Decreases in cytochrome oxidase reaction product became more prominent at 1 hour of reperfusion in the areas of the dentate gyrus, CA_1, CA_2, CA_3, cortex and thalamus followed by a further decline at 24 hours of reperfusion (Fig. 13). In 4 week old rats, there was a subtle decrease of enzyme reaction in the dentate gyrus both during and immediately after hypoxia. At 24 hours of reperfusion, the decrease in cytochrome oxidase reaction product became evident in the areas of dentate gyrus, CA_1 and CA_2 but not CA_3 (Fig. 14).

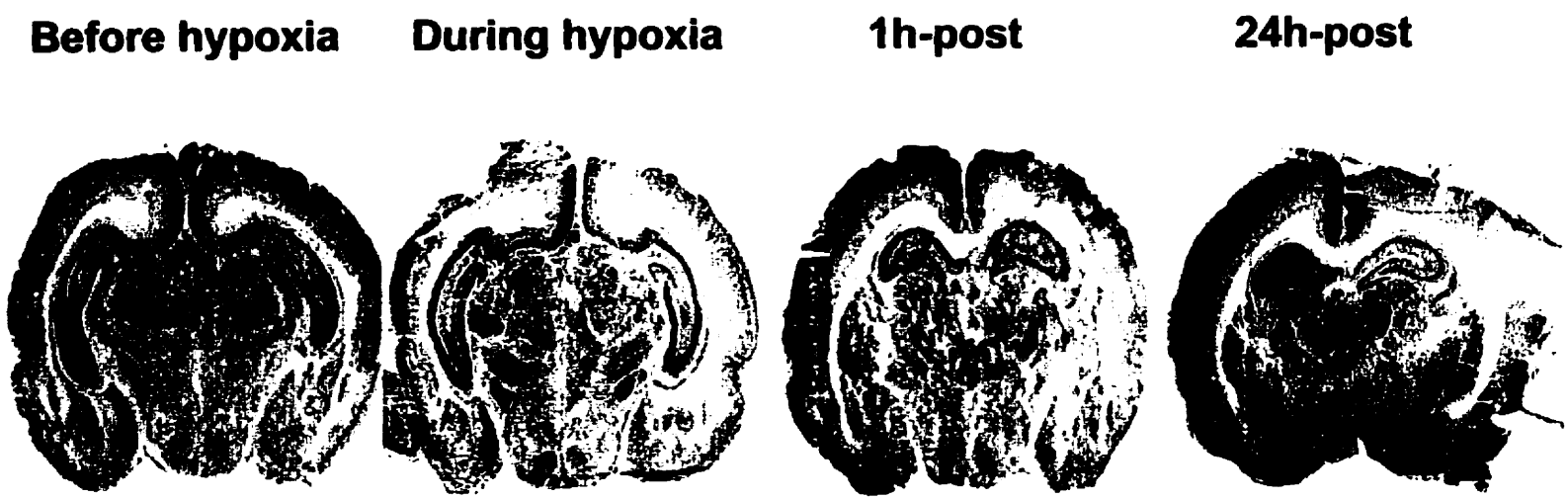

Fig. 13. Hypoxic/ischemic changes in cytochrome oxidase in 1 week old rats. At 1 hour of reperfusion, a decrease in cytochrome oxidase reaction product occurs in the hemisphere ipsilateral to the carotid occlusion in the hippocampus, cortex and thalamus followed by a further decline at 24 hours of reperfusion.

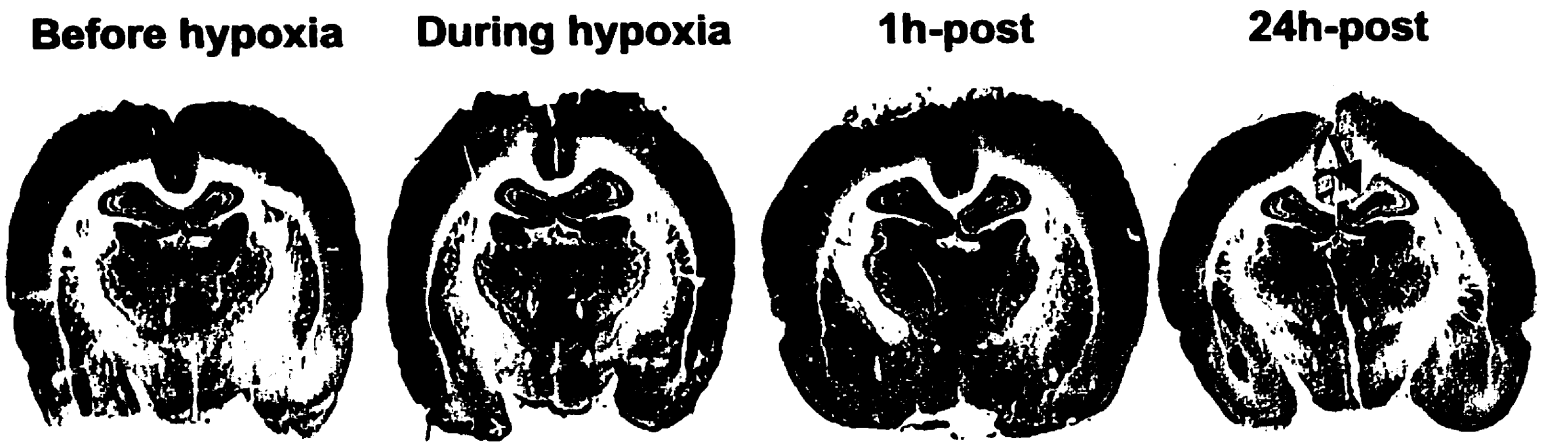

Fig.14. Hypoxic/ischemic changes in cytochrome oxidase in 4 week old rats. At 24 hours of reperfusion, a decrease in cytochrome oxidase reaction product becomes apparent in the hippocampus, particularly in the CA_1 sector (arrow)

PATHOLOGICAL CHANGES

In general, there were differences in hypoxic/ischemic changes in 1 and 4 week old brains. Punctate chromatin, pyknosis and Annexin V labeled cells were observed more frequently in 1 week old rats than 4 week old rats in the ipsilateral hemisphere 24 hours after hypoxia/ischemia whereas eosinophilic cells were observed more frequently in 4 week old brain.

1) 1 week old rats

Evidence of edema was one of the first tissue changes observed in neonatal brain during and immediately after hypoxia. Almost the entire hemisphere ipsilateral to the occlusion at the level of mid thalamus appeared pale with a distinct boundary between the pale and normal tissue. After 24 hours post hypoxia, 7/7 rats exhibited massive infarction in the ipsilateral hemisphere at the level of middle cerebrum. Cells with punctate chromatin or pyknotic nuclei were distributed throughout the territory of the right common carotid artery (Fig. 15). In the hippocampus, dying cells were observed in the dentate gyrus, CA_1, CA_2 and CA_3 sectors. Cells double labeled with Annexin V (Fig. 16) and propidium iodide were observed more frequently in the ipsilateral cortex and thalamus in 2/5 rats during hypoxia, in 4/9 rats at 1 hour of reperfusion and in 7/7 rats at 24 hours post hypoxia.

2) 4 week old rats

On H & E stained sections, there were no obvious morphological changes during hypoxia or at 1 hour of reperfusion. Histological changes were detected in the ipsilateral hemisphere at 24 hours of reperfusion. At the level of middle cerebrum, 2/6 brains exhibited large areas of infarction in the ipsilateral hemisphere. The other 4/6 brains exhibited selective cellular necrosis in the hippocampus or cortex, particularly in CA_1. In 4 week old brain, there was a predominance of eosinophilic cells and fewer cells with pyknotic or punctate nuclei compared to 1 week old brain. In 3/6 rats, cells with labeling positively for Annexin V were observed in the ipsilateral cortex, thalamus or hypothalamus but only after 24 hours of reperfusion. However, these Annexin V labeled cells were not co-labeled with propidium iodide.

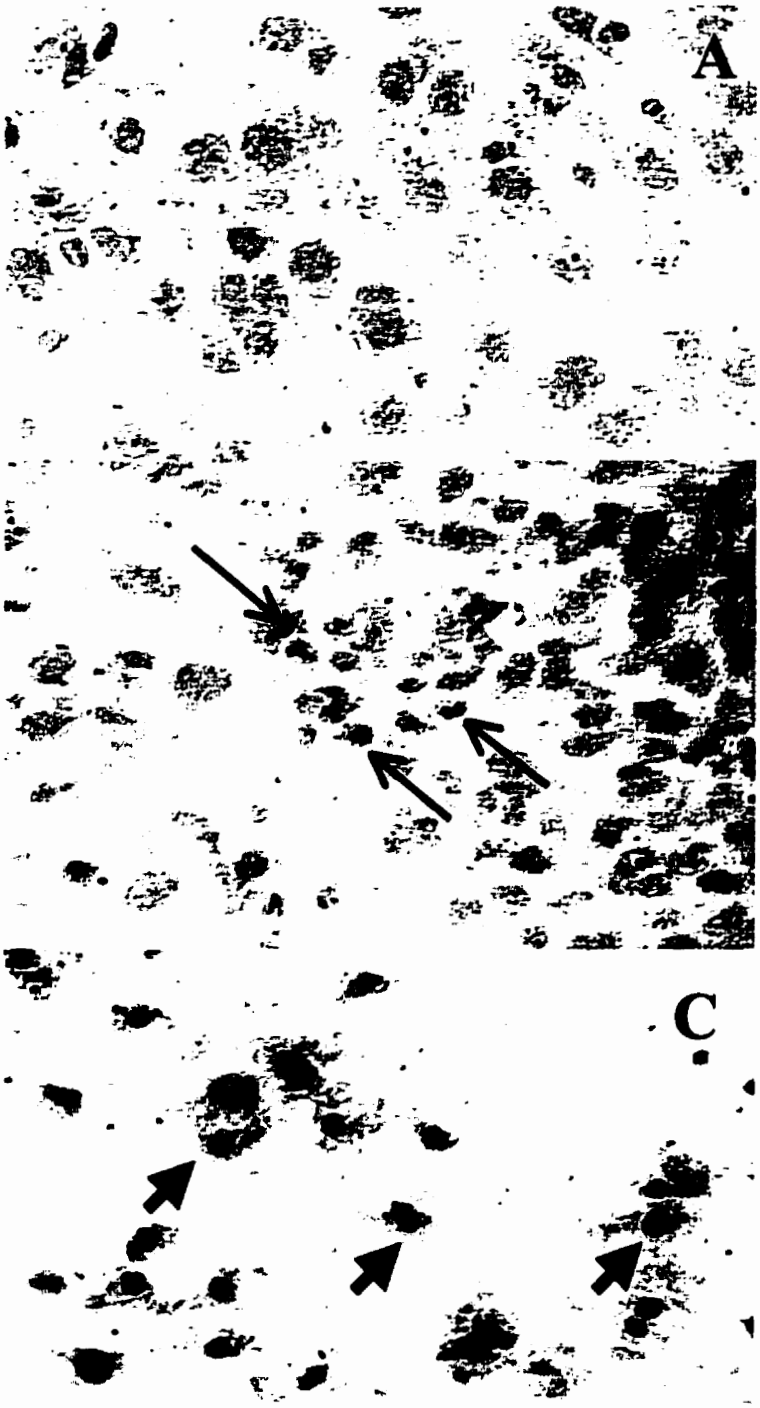

Fig. 15. Micrographs showing pathological changes in the cerebral cortex of 1 week old rats at 24 hours of reperfusion (H & E). (A) showing normal nuclei in a sham control; (B) showing the punctate chromatin (long arrow) in the cortex ipsilateral to the occlusion; (C) showing pyknotic nuclei (short arrow) in the cortex ipsilateral to the occlusion.

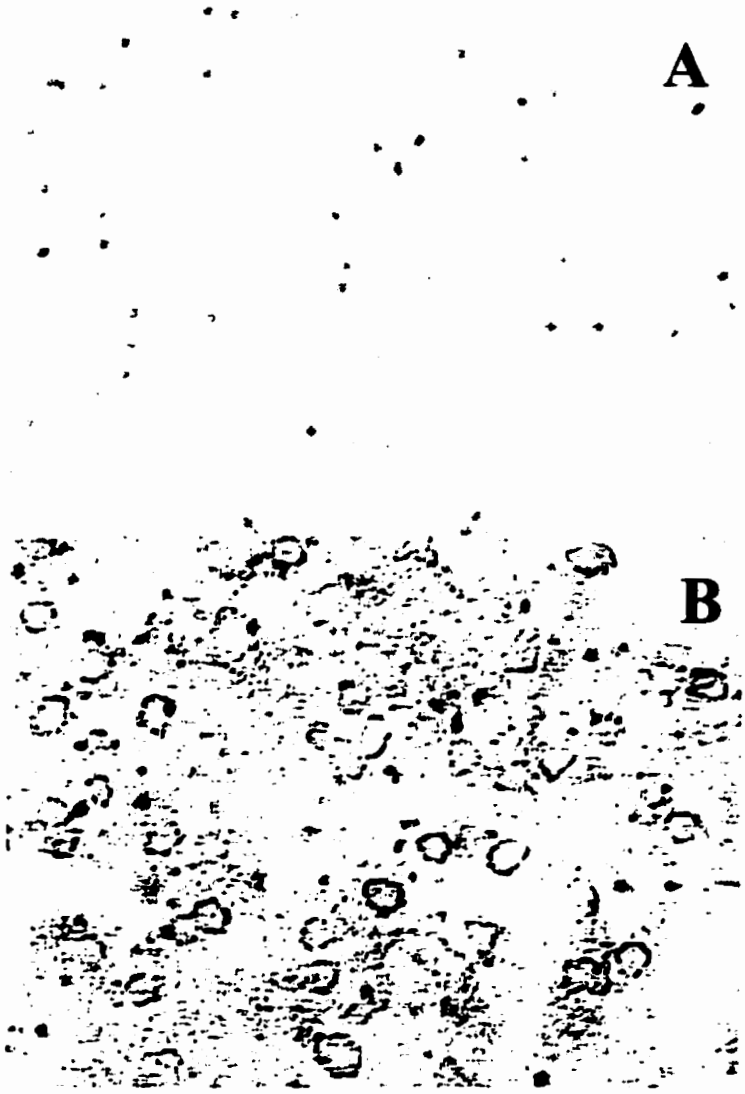

Fig. 16. Micrographs showing Annexin V labeling in the cortex contralateral (A) and ipsilateral (B) to the occlusion at 24 hours of reperfusion in 1 week old rats. Dying cells were labeled with Annexin V around the cellular membrane.

CORRELATION OF MR CHANGES WITH TISSUE ALTERATIONS

1) Correlation of changes in T_2 with alterations in brain water

In general, the appearance of hyperintensity in TW images at 24 hours of reperfusion corresponded to the increase in brain water in both 1 and 4 week old rats (Table 1). T_2 changes before, during and after hypoxia/ischemia corresponded well to the alterations in brain water in 1 week old rats but only partially in 4 week old rats. In 4 week old rats, elevation in brain water occurring during hypoxia-ischemia and immediately after the termination of hypoxia was not detected in TW images until 24 hours after hypoxia. In addition, correlation between T_2 and brain water content or specific gravity demonstrated a strong linear relationship at 1 and 24 hours of reperfusion in 1 week old rats (Fig. 17A, B). In 4 week old rats, the correlation of T_2 with brain water content in the anterior cerebrum was significant whereas that between T_2 and brain specific gravity in the posterior cerebrum was not (Fig. 18A, B).

2) Correspondence of changes in diffusion-weighted images to alterations in Na^+-K^+-ATPase

In general, the appearance of hyperintensity in DW images at 24 hours of reperfusion corresponded to the decline in Na^+-K^+-ATPase reaction in both 1 and 4 week old rats (Table 1).The temporal changes in DW images following the onset of hypoxia/ischemia corresponded to the changes in Na^+-K^+-ATPase in 1 week old rats. The correspondence was less consistent in 4 week old rats. In 4 week old rats, there was a similar correspondence of changes in DW images to Na^+-K^+-ATPase during and 24 hours after hypoxia/ischemia although there were no detectable hyperintensity in the DW

images at 1 hour of reperfusion despite a significant decrease in Na^+-K^+-ATPase ipsilaterally.

3) Correlation of MR hyperintensity areas with cell death or infarction

In 1 week old rats, the mean area of hyperintensity in DW images and TW images at 24 hours of reperfusion was very close to the mean area of infarction (Table 1). There was also a linear correlation between the hyperintensity areas in TW and DW images at 24 hours of reperfusion ($r = 0.7$, $P < 0.05$). Furthermore, the areas of hyperintensity in both TW ($r= 0.5$, $P < 0.05$) and DW images ($r = 0.9$, $P < 0.05$) (Fig. 19) correlated with the areas of infarction.

In 4 week old rats, there was a linear correlation between area of infarction and area of hyperintensity in TW images ($r = 0.9$, $P < 0.05$) and area of hyperintensity in DW images ($r = 0.9$, $P < 0.05$). The hyperintensity area in TW images corresponded to the area of infarction whereas hyperintensity area of DW images was larger than the area of infarction. Areas of selective cellular necrosis without an infarction or a visible loss of H & E staining were not measurable with the MCID system.

4) Correlation of changes in cytochrome oxidase with MR changes or cell death

In both age groups, the area with a decrease in cytochrome oxidase reaction product at 24 hours of reperfusion corresponded well to the area of hyperintensity in DW images ($r = 0.97$ in 1 week old rats; $r = 0.8$ in 4 week old rats, $P < 0.05$) and TW images ($r = 0.5$ in 1 week old rats; $r = 0.8$ in 4 week old rats, $P < 0.05$) (Table 1). Furthermore,

the area with a decrease in cytochrome oxidase reaction product at 24 hours of reperfusion correlated well with the area of infarction in both 1 week ($r = 0.8$, $P < 0.05$) (Fig. 20) and 4 week old rats ($r = 0.7$, $P < 0.05$) (Table1).

Table 1. Comparison of changes in MR images with alterations in specific gravity, Na^+-K^+-ATPase, cytochrome oxidase and pathology 24 hours after hypoxia/ischemia in 1 week and 4 week old rats

	1 week old rats	4 week old rats
T_2 hyperintensity area[a]	37% ± 0.11	6% ± 0.07
DW hyperintensity area[a]	40% ± 0.14	18% ± 0.17
Area with a reduction in Na+-K+-ATPase [a]	39% ± 0.08	27% ± 0.16
Area with a reduction in cytochrome oxidase [a]	42% ± 0.10	21% ± 0.17
Area of Infarction[a]	37% ± 0.16	8% ± 0.13
Decrease in specific gravity (ispsilateral)[b]	0.67% ± 0.004	0.25% ± 0.002

a) data are presented as a percentage of an entire brain slice at the level of mid thalamus; b) data are presented as a percentage of decrease in specific gravity in the ipsilateral cerebrum compared to the data in the cerebrum contralateral to the carotid occlusion at the level of posterior thalamus.

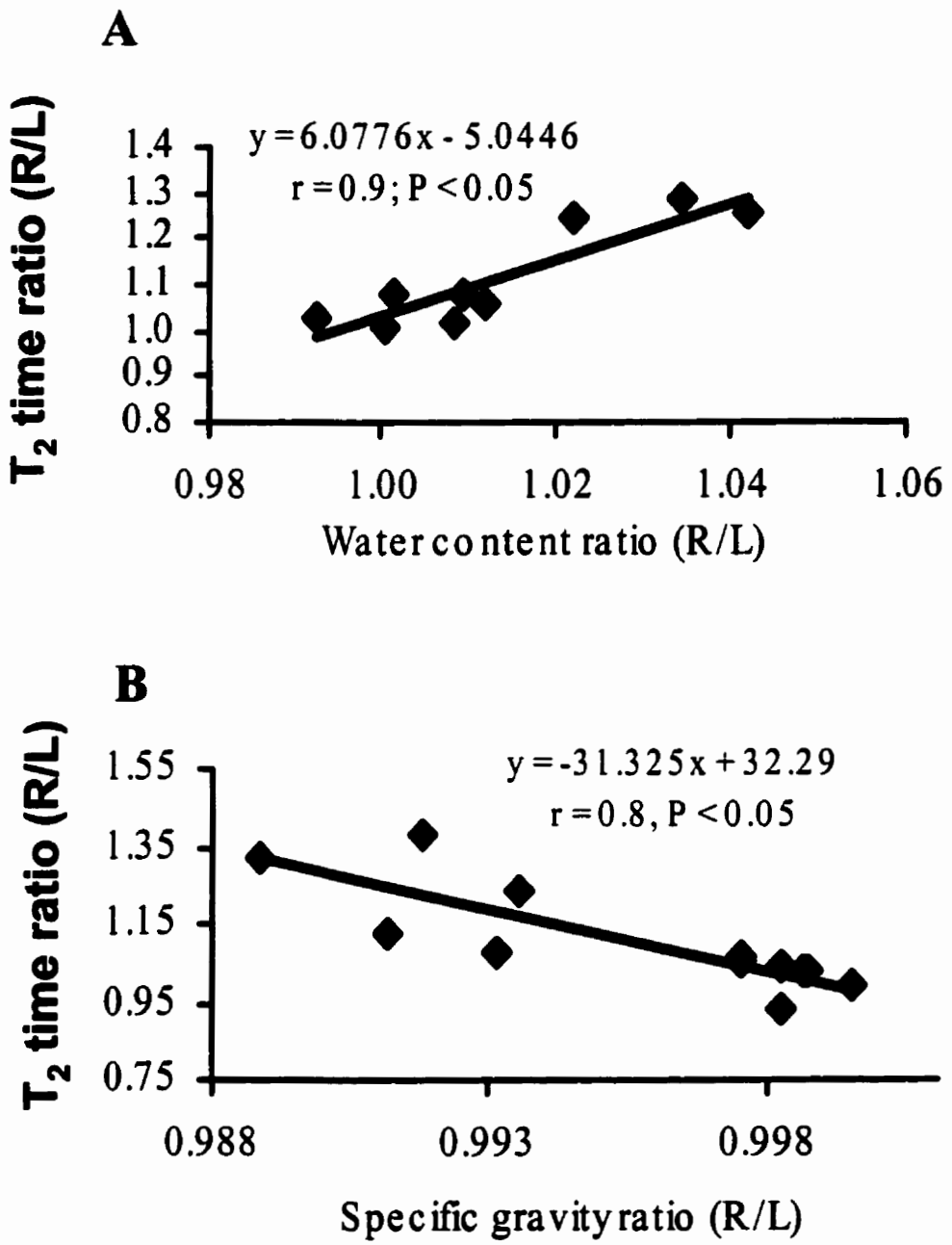

Fig. 17. Correlation of T_2 relaxation times with brain water at 1and 24 hours following hypoxia/ischemia in 1 week old rats where brain water in the anterior or posterior cerebrum was assessed using a measure of water content (A) (dry/wet weight) or specific gravity (B), respectively. All the data are presented as the mean ratio of values in the ipsilateral/contralateral hemisphere (R/L).

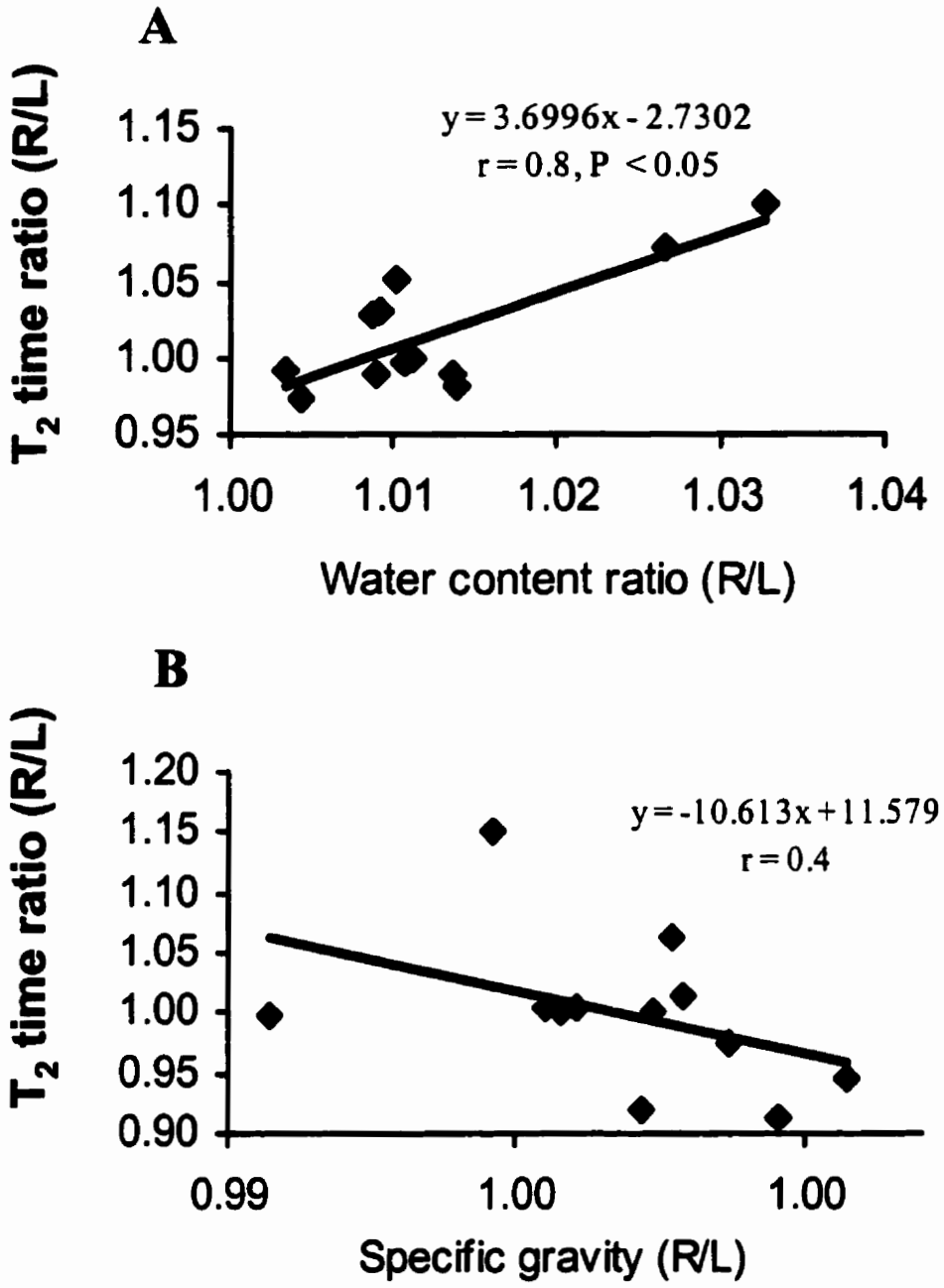

Fig. 18. Correlation of T_2 relaxation times with brain water at 1and 24 hours following hypoxia/ischemia in 4 week old rats where brain water in the anterior or posterior cerebrum was assessed using a measure of water content (A) (dry/wet weight) or specific gravity (B), respectively. All the data are presented as the mean ratio of values in the ipsilateral/contralateral hemisphere (R/L).

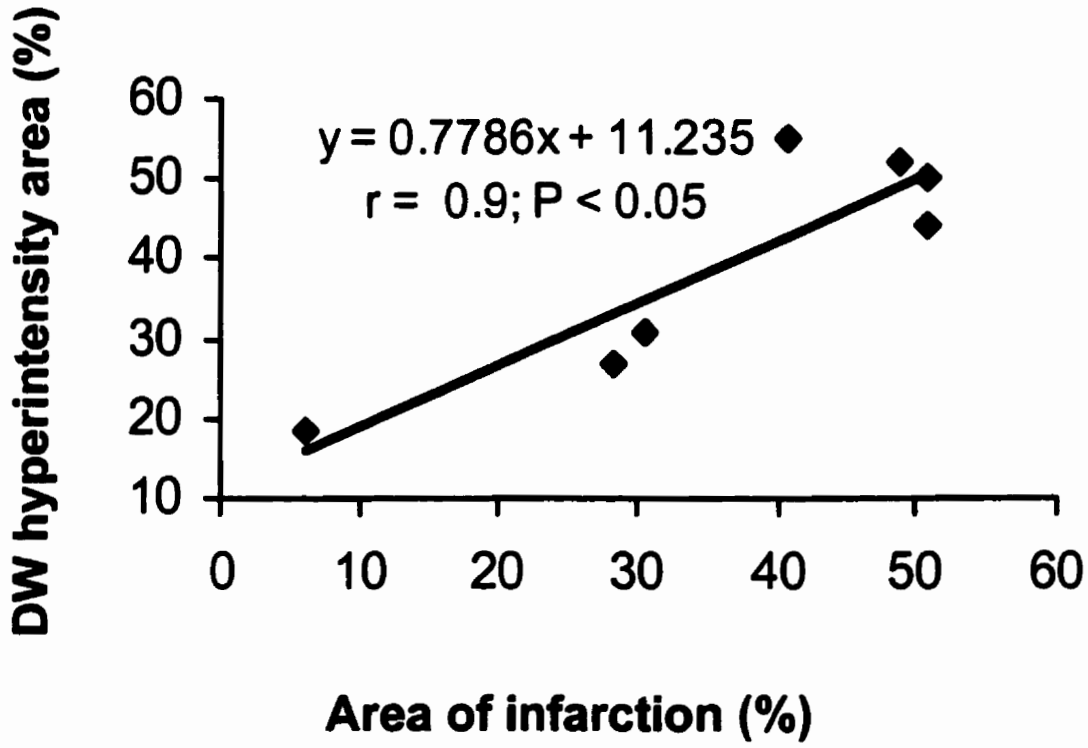

Fig. 19. Correlation of hyperintensity area of diffusion-weighted images at 24 hours of reperfusion with area of infarction in 1 week old rats. Area of hyperintensity or infarction is presented as a percentage of the entire brain slice.

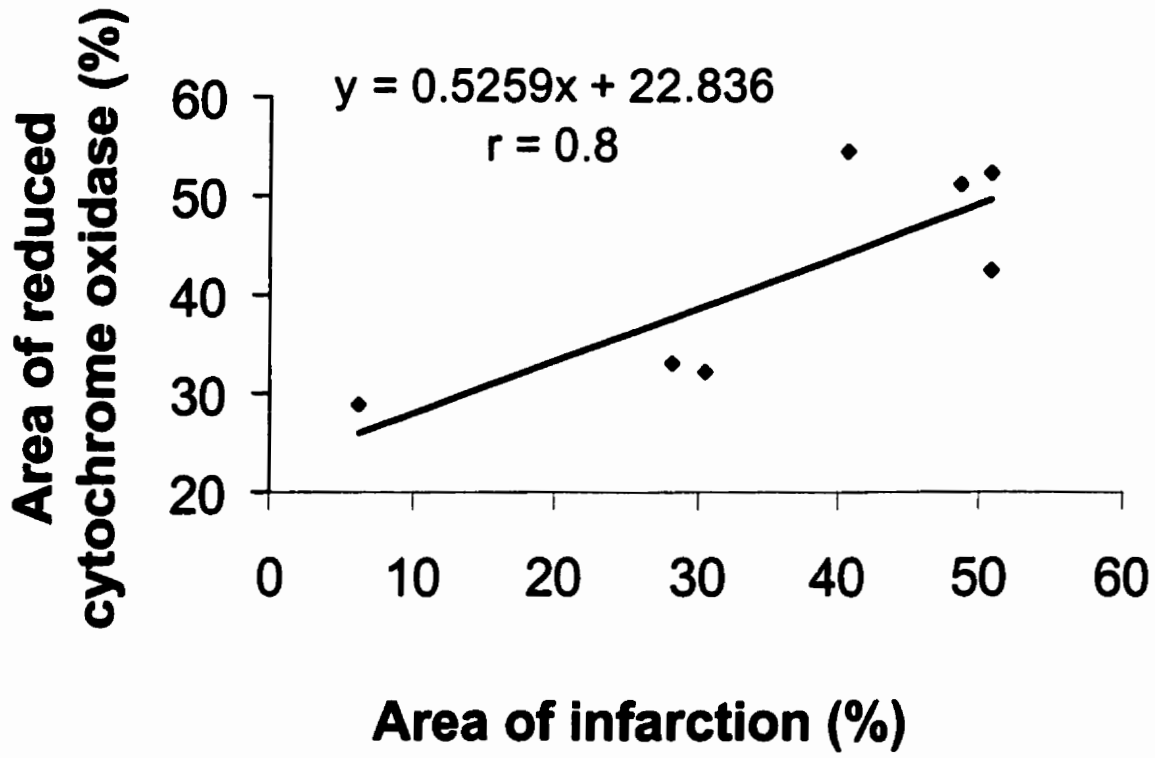

Fig. 20. Correlation of area of reduced cytochrome oxidase at 24 hours of reperfusion with area of infarction in 1 week old rats. Area with a reduction in cytochrome oxidase reaction product or area of infarction is presented as a percentage of the entire brain slice.

DISCUSSION

Both DW and TW imaging have been used extensively to detect cerebral hypoxic/ischemic changes in neonatal and young rats (Ning *et al.*, 1999; Tuor *et al.*, 1998). Although the onset of imaging changes and their recovery following an episode of hypoxia/ischemia are suggested to be age-related and due to differences in brain water or extracellular space, there is no direct evidence to confirm this. A unique feature of the present study is that we investigated the temporal and spatial profiles of MR changes and their tissue correlates at both early and later stages of the hypoxic/ischemic insults. The results support our hypothesis that changes in T_2 correspond to alterations in brain water content and changes in DW images correspond to the alterations in Na^+-K^+-ATPase in hypoxia/ischemia in 1 week old rats but only partially in 4 week old rats.

INTERPRETATION OF DIFFUSION-WEIGHTED IMAGES IN HYPOXIA/ISCHEMIA

A) Age difference in the onset of brightness in diffusion-weighted images in hypoxia/ischemia

The increased intensity in DW images originates from a reduction in the diffusion of water in tissue. Compared to traditional MR imaging, DW imaging is more sensitive for detecting early disturbances in energy metabolism before complete depletion of energy substrates and irreversible cellular damage (Hossmann *et al.*, 1994). Early changes in ADC or the brightness in DW images occurs within minutes after the onset of ischemia in an adult rat MCAO model (Hoehn Berlage *et al.*, 1995). We found that the onset of DW changes in hypoxia/ischemia was different in neonatal and young brain.

Hyperintense DW images of the hemisphere ipsilateral to the carotid occlusion occurred as early as 10 – 15 minutes after the onset of hypoxia in 4 week old rats whereas it was between 30 - 45 minutes in 1 week old rats. Since the rats in both age groups suffered the same degree of hypoxia (8% oxygen), the difference in the onset of DW changes was somehow age-related. There are at least three possible mechanisms contributing to the age dependence of the onset of DW hyperintensity. First, developmental differences in cerebral energy metabolism might contribute to the delayed appearance of hyperintensity in DW images in 1 week old rats. Both oxygen and glucose consumption by the brain undergo a sigmoid rise between birth and adulthood (Tuor, 1991). In addition, neonatal brain can take up and use other energy substrates generated during hypoxia, such as lactate and ketone bodies, which in adults cause adverse effects such as acidosis (Nehlig and Pereira de Vasconcelos, 1993). The lower demand for glucose and more flexible use of energy sources in neonatal brain assure that the level of ATP is less disturbed during hypoxia/ischemia compared to young brains. Second, the volume of the extracellular space in immature brain is high and it gradually decreases as the brain matures (van der Toorn *et al.*, 1996; Lehmenkuhler *et al.*, 1993). Thus, the shrinkage of the extracellular compartment in hypoxia/ischemia may not be evident in neonatal brain due to a higher buffering capacity of the extracellular space in response to a disturbance of ion balance during hypoxia/ischemia. Vorisek and Sykova (1997) reported that the younger the animal, the longer the latency for changes in extracellular space and tortuosity in anoxia in developing rats. It is believed that the shrinkage of extracellular space is the major reason for the reduction of ADC or the corresponding increase in intensity in DW images (Verheul *et al.*, 1994; van der Toorn *et al.* 1996; van Lookeren Campagne *et al.*, 1994).

Third, immunohistochemical techniques have demonstrated that the amount of Na^+-K^+-ATPase in the rat brain is very low at postnatal day 7 and increases remarkably between postnatal day 7 - 35 (Fukuda and Prince, 1992). Using histochemical methods, similar changes with age were found in our study where the reaction product for Na^+-K^+-ATPase in 4 week old brain was much greater than that in 1 week old brain despite much shorter incubation times. A lower basal level or Na^+-K^+-ATPase enzyme activity in neonatal brain indicates a lower ATP requirement to maintain ion pump function and cell volume homeostasis, thereby prolonging the onset of shortages in ATP.

B) Correspondence of changes in diffusion-weighted images to alterations in Na^+-K^+-ATPase

A decrease in extracellular space has been believed to be a major cause of the reduction of ADC in cerebral ischemia (van der Toorn *et al.*, 1996). It is also generally accepted that cell volume is primarily regulated by Na^+-K^+-ATPase within the membrane. Thus, we speculated that the decrease in Na^+-K^+-ATPase activity provide an index of a decrease in extracellular space. Compared to methods that provide an assessment of changes in extracellular space such as electrical impedance (van Lookeren Campagne *et al.*, 1994), the histochemical technique we used has advantages of saving time and providing spatial information regarding changes in Na^+-K^+-ATPase. The major concern about the histochemical staining method is that it may be non-specific. In our studies, levamisole was added to suppress the non-specific staining for alkaline phosphatase and the reaction product was stabilized with the addition of DMSO

(Mayahara *et al.*, 1980). In addition, a variety of control experiments in our studies demonstrated that the staining with our methods was specific for Na^+-K^+-ATPase.

In 1 week old rats, the trend of changes in DW images over the time course of hypoxia/ischemia experiments corresponded to the alterations in Na^+-K^+-ATPase. A similar correlation has been reported in an adult MCAO model (Mintorovitch *et al.*, 1994). In addition, ADC decreases have been observed following the intracerebral administration of ouabain, an inhibitor of Na^+-K^+-ATPase (Benveniste *et al.*, 1992). These results support the assumption that a decrease of ADC in DW images is related to the decrease in membrane Na^+-K^+-ATPase function. The disturbance in Na^+-K^+-ATPase function would result in water shift from the extracellular space into intracellular space, a shrinkage of the extracellular space and a resulting in a decrease in ADC. The intensity for Na^+-K^+-ATPase histochemical reaction product reflects the activity and density of Na^+-K^+-ATPase in brain tissue. Does the reduction of Na^+-K^+-ATPase reaction product shown at later stage of reperfusion result solely from the decrease in enzyme density due to the loss of cells? Biochemical analysis was demonstrated that hypoxia and/or ischemia results in a decrease in Na^+-K^+-ATPase activity as early as 1 hour after hypoxia until 24 hours of reperfusion (Groenendaal *et al.*, 1990; Stanimirovic *et al.*, 1997; Yang *et al.*, 1992). Therefore, hyperintensity in DW images during and following hypoxia/ischemia is likely related at least in part to a decline in Na^+-K^+-ATPase activity.

However, such a correlation was not in complete agreement with the changes observed in 4 week old brains. In 4 week old rats, DW images had a remarkable recovery at 1 hour of reperfusion but the decreased reaction product for Na^+-K^+-ATPase remained in the ischemic hemisphere. This indicates that there are other mechanisms responsible

for the changes of ADC in 4 week old brain subjected to hypoxia/ischemia. 2-[^{19}F]luoro-2-deoxyglucose-6-phosphate (2FDG-6P) has been employed as a compartment-specific marker in normal and globally ischemic rat (Duong *et al.*, 1998). A similar decrease in the intracellular and extracellular ADC was found in cerebral ischemia both *in vivo* and *in vitro*, suggesting that in addition to alterations in the extracellular space, changes in water diffusion through the intracellular compartment play an important role in the ADC changes observed following ischemic insults. The diffusion of intracellular water is more restricted than that of the extracellular water because of its interaction with intracellular organelles and macromolecules. Also, acidosis, degradation of the cytoskeleton, changes in membrane water permeability and alterations in intracellular transport system have all been suggested to contribute to the reduction in ADC (Duong *et al.*, 1998; Hossmann *et al.*, 1994; Zhong *et al.*, 1993). Recent studies demonstrated that the areas of reduction in ADC were larger than those of ATP depletion but corresponded well to those of acidosis in an adult MCAO model (Hossmann *et al.*, 1994; Kohno *et al.*, 1995). Thus, the recovery of DW images in 4 week old rats might be due to the recovery of acidosis and other associated biochemical changes instead of the extracellular space. Correlation of DW changes with the tissue alteration in hypoxia/ischemia needs to be further investigated.

C) Correlation of changes in diffusion-weighted images with infarction

In both age groups, the areas of hyperintensity in DW images at 24 hours of reperfusion were smaller than those during hypoxia but corresponded well to the areas of infarction. This implies that the areas of hyperintensity, which were reversible after 24

hours of reperfusion might represent a penumbral region where cell injury may be reversible upon recirculation whereas an area without a recovery of hyperintensity changes appears to form the core of the infarction. Indeed, several studies have demonstrated that there is a graded reduction in ADC and blood flow from the periphery of the insult to the core of the infarction and regions with a mild reduction in ADC could be located within the penumbra (Dijkhuizen *et al.*, 1997; Hoehn Berlage *et al.*, 1995; Pierce *et al.*, 1997). Thus, DW imaging is likely helpful in detecting early ischemic changes and monitoring the efficiency of therapy within the penumbra in stroke patients. The strong linear correlation between areas of DW hyperintensity at 24 hours of reperfusion and the areas of infarction implies that DW changes 24 hours after ischemia/hypoxia reflect cell death in the tissue.

INTERPRETATION OF T_2 CHANGES IN HYPOXIA/ISCHEMIA

A) Age difference in the onset of T_2 changes in hypoxia/ischemia

The signal on TW images originates from the relaxation of water in the tissue and the intensity within TW images is determined by the proton density and T_2 relaxation time. The onset of hypoxia/ischemia-induced changes in T_2 occurred much earlier in 1 week old rats than in 4 week old rats. We speculated that T_2 was normal because brain water was unchanged in the more mature brain early in hypoxia/ischemia. However, both dry/weight and percoll methods demonstrated that there was an elevation of brain water already by the end of 30-minute-hypoxia which persisted until at least 24 hours after hypoxia. Possible explanations for a delayed T_2 increase despite increases in brain water will be discussed below. The onset of T_2 changes corresponded well to the disturbance in

water and ion balance in 1 week old brain and the presence of irreversible cell injury or death in 4 week old brain indicated as decreased reaction product for cytochrome oxidase or cell death morphologically. This suggests that the onset of changes in T_2 in hypoxia/ischemia reflect potentially reversible cellular changes in neonatal brain and irreversible cellular damage in young rats.

B) Correlation of changes in T_2 and alterations in brain water in hypoxia/ischemia

The high T_2 occurring following cerebral ischemia has been generally thought to be due to an elevation of water content (Loubinoux *et al.*, 1997; Mintorovitch *et al.*, 1991; Mathur de Vre, 1984). Our results demonstrate that changes in TW images are in agreement with the trend of changes in brain water in both early and later stages of hypoxia/ischemia in 1 week old rats. This supports the assumption that the hyperintensity shown on TW images during and following ischemia/hypoxia results from the increased content of brain water (Tuor *et al.*, 1998).

However, the changes in the net bulk of water can not explain all the results observed in young rats. In 4 week old rats, T_2 changes were delayed by up to 24 hours of reperfusion despite significant increases in water content or decreases in specific gravity early during and soon after hypoxia/ischemia. Why does TW imaging detect the elevation of brain water soon after the onset of hypoxia/ischemia in 1 week but not in 4 week old rats? The water content continues to decrease with brain maturation. In control groups, 1 week brain had a much higher level of water content than the 4 week old brain. Even though the water content in 4 week old brain was significantly elevated during hypoxia,

the total water content in the ipsilateral hemisphere was still much lower than that in 1week old brain. This means that the absolute proton density and the total sum of magnetization in the transverse direction is smaller in 4 week old rats compared to 1 week old rats. If the net magnetization sensed by the RF coil is not enough to reach the threshold for the differentiation of the brightness in the pixels, then images would not show any hyperintensity even though brain water increases in the tissue. Another possible mechanism is an age dependent difference in the intrinsic microscopic magnetic environment. Water in the body can exist in a free form or a bound form. In fact, the T_2 signal of a biological tissue reflects the T_2 relaxation of water in a complex environment where it interacts with other macromolecules, such as protein and lipids. The surrounding macromolecules can interact with the water molecules resulting in a fluctuation or inhomogeneity of the local magnetic field. Increase in bound water is associated with shorter T_2 values because of a greater fluctuation in the local magnetic field (Chakeres and Schmalbrock, 1992). On the other hand, an increase in free water is associated with a longer T_2 value because of the homogeneity of local magnetic field. Therefore, the ratio of free water/bound water determines the net T_2 in biological tissues (Mathur de Vre, 1984). If a decreased T_2 originating from an increase in bound water is equal to the increased T_2 originating from an increase in free water, then, there are no net changes in TW images. Therefore, the absence of T_2 changes in 4 week old rats during early periods of hypoxia/ischemia might be the result of an increase in both bound and free water content.

C) Correlation of T_2 changes with infarction

Despite its insensitivity to detection of early changes in brain water in 4 week old rats, the T_2 changes at a later stage of reperfusion correlated well with the areas of infarction or areas with decreased cytochrome oxidase reaction product in both 1 week and 4 week old rats. This suggests that the changes in T_2 24 hours after hypoxia/ischemia detect cell death in tissue.

CHANGES IN CYTOCHROME OXIDASE IN HYPOXIA/ISCHEMIA

Cell death was evident throughout the hippocampus occurring in the dentate gyrus, CA_1, CA_2 and CA_3 in 1 week old rats whereas it occurred most commonly in CA_1 in 4 week old rats. This is consistent with previous reports that the CA_1 is particularly vulnerable to hypoxia or ischemia in mature brain (Towfighi *et al.*, 1997; Abe *et al.*, 1998). Consistent with our results, previous pathological studies have demonstrated that the relative vulnerability of various hippocampal regions is equivalent early postnatally and high susceptibility of CA_1 to hypoxia was approached by postnatal day 21 (Towfighi *et al.*, 1997). The underlying mechanisms of different selective susceptibility of the hippocampus to hypoxia in immature and mature brains are unclear. In our studies, we found that the regional distribution of cell death correlated well with the decrease in cytochrome oxidase reaction at 24 hours of reperfusion in both groups. This suggests that the age-dependent selective vulnerability of the hippocampus to hypoxia is somehow related to differences in mitochondrial function. Impairment of cytochrome oxidase indicates that the pathway of oxidative phosphorylation is interrupted with the consequence of a decrease in the production of ATP and a decrease in the mitochondrial transmembrane potential (Balaban, 1990). If the generation of ATP in the mitochondria

continues to decrease and becomes insufficient to maintain cellular function (ATP depletion), irreversible cell death occurs eventually. Since the decreased intensity for cytochrome oxidase reaction product might also result from the loss of enzyme density due to cell death at the later stage of reperfusion, cytochrome oxidase activity needs to be further investigated using biochemical analysis.

SUMMARY AND CONCLUSIONS

This study demonstrated that changes in DW and TW images following hypoxic/ischemic corresponded quite well to tissue changes examined in 1 week old rats but only corresponded partially in 4 week old rats:

1) The hypoxic/ischemic changes in T_2 correlated well with alterations in brain water in 1 week old rats, but early elevations in brain water in 4 week old rats could not be detected by TW imaging technique.

2) The hypoxic/ischemic changes in the DW changes corresponded to alterations in brain Na^+-K^+-ATPase in 1 week old rats; however, the persistent decreases in Na^+-K^+-ATPase occurring immediately after hypoxia/ischemia in 4 week old rats were not reflected in the DW images.

3) Hyperintensity areas of DW and TW occurred as early as 30-45 minutes after the onset of hypoxia/ischemia in 1 week old rats whereas in 4 week old rats hyperintensity changes in DW images appeared 10-15 minutes after the onset of hypoxia/ischemia but the T_2 changes occurred at 24 hours of reperfusion. The onset of T_2 changes corresponded to the the disturbance in water dynamics in neonatal brain and the presence of cell death in 4 week old brain.

4) The hyperintense areas in DW images without secondary changes at 24 hours of reperfusion suggest that these might be penumbral regions whereas those areas with a secondary reappearance of hyperintensity correspond well to the areas of infarction.

5) Changes in DW and TW images after 24 hours of reperfusion reflect infarction in both age groups.

6) Cytochrome oxidase was impaired in hypoxia/ischemia in both age groups and its impairment possibly contributed to the selective cell death observed in the hippocampus.

In general, the hypoxic/ischemic MR imaging changes are consistent with alterations in brain water and Na^+-K^+-ATPase in neonatal brain but not in young brain. This implies that an age-related difference in the ischemic tissue might reduce the visibility of hypoxic/ischemic MR changes in young brain. The early T_2 changes reflect reversible changes in water dynamics in neonatal brain whereas the later T_2 changes reflect the presence of cell death in both neonatal and young brain. Compared to traditional MR imaging techniques, DW imaging detects early hypoxic/ischemic changes, some of which are possibly related to the penumbra.

REFERENCES

Abe K, Kawagoe J, Aoki M, Kogure K, Itoyama Y. Stress protein inductions after brain ischemia. *Cell Mol Neurobiol* 1998;**18**:709-719.

Agrawal HC, Davis JM, Himwich WA. Developmental changes in mouse brain weight, water content and free amino acids. *J Neurochem* 1968;**15**:917-923.

Allegrini PR, Sauer D. Application of magnetic resonance imaging to the measurement of neurodegeneration in rat brain: MRI data correlate strongly with histology and enzymatic analysis. *Magn Reson Imaging* 1992;**10**:773-778.

Balaban RS. Regulation of oxidative phosphorylation in the mammalian cell. *Am J Physiol* 1990;**258**:C377-C389.

Balayer L, Busto R, Zhao WZ, Ginsberg MD. Quantitative evaluation of blood-brain barrier permeability following middle cerebral artery occlusion in rats. *Brain Res* 1996;**739**:88-96.

Barone FC, Clark RK, Feuerstein G, Lenkinski RE, Sarkar SK. Quantitative comparison of magnetic resonance imaging and histological analyses of focal ischemic damage in the rat. *Brain Res Bull* 1991;**26**:285-291.

Benveniste H, Hedlund LW, Johnson GA. Mechanism of detection of acute cerebral ischemia in rats by diffusion-weighted magnetic resonance microscopy. *Stroke* 1992;**23**:746-754.

Boisvert DP, Handa Y, Allen PS. Proton relaxation in acute and subacute ischemic brain edema. *Adv Neurol* 1990;**52**:407-413.

Bradbury MW, Cserr HF, Westrop RJ. Drainage of cerebral interstitial fluid into deep cervical lymph of the rabbit. *Am J Physiol* 1981;**240**:F329-F336

Brasch RC. Work in progress: methods of contrast enhancement for NMR imaging and potential applications. A subject review. *Radiology* 1983;**147**:781-788.

Brightman MW, Hori M, Rapoport SI, Reese TS, Westergaard E. Osmotic opening of tight junctions in cerebral endothelium. *J Comp Neurol* 1973;**152**:317-325.

Brody BA, Kinney HC, Kloman AS, Gilles FH. Sequence of central nervous system myelination in human infancy. I. An autopsy study of myelination. *J Neuropathol Exp Neurol* 1987;**46**:283-301.

Cala PM, Anderson SE, Cragoe-EJ J. Na/H exchange-dependent cell volume and pH regulation and disturbances. *Comp Biochem Physiol A* 1988;**90**:551-555.

Cameron IL, Ord VA, Fullerton GD. Characterization of proton NMR relaxation times in normal and pathological tissues by correlation with other tissue parameters. *Magn Reson Imaging* 1984;**2**:97-106.

Chakeres DW, Schmalbrock P. Fundamentals of magnetic resonance imaging. Baltimore: Williams & Wilkins, 1992.

Dijkhuizen RM, Berkelbach van der Sprenkel JW, Tulleken KA, Nicolay K. Regional assessment of tissue oxygenation and the temporal evolution of hemodynamic parameters

and water diffusion during acute focal ischemia in rat brain. *Brain Res* 1997;**750**:161-170.

Duong TQ, Ackerman JJ, Ying HS, Neil JJ. Evaluation of extra- and intracellular apparent diffusion in normal and globally ischemic rat brain via ^{19}F NMR. *Magn Reson Med* 1998;**40**:1-13.

Eveloff JL, Warnock DG. Activation of ion transport systems during cell volume regulation. *Am J Physiol* 1987;**252**:F1-10.

Fukuda A, Prince DA. Postnatal development of electrogenic sodium pump activity in rat hippocampal pyramidal neurons. *Dev Brain Res* 1992;**65**:101-114.

Fullerton GD, Potter JL, Dornbluth NC. NMR relaxation of protons in tissues and other macromolecular water solutions. *Magn Reson Imaging* 1982;**1**:209-226.

Gill R, Sibson NR, Hatfield RH, et al. A comparison of the early development of ischemic damage following permanent middle cerebral artery occlusion in rats as assessed using magnetic resonance imaging and histology. *J Cereb Blood Flow Metab* 1995;**15**:1-11.

Go KG. The normal and pathological physiology of brain water. *Adv Tech Stand Neurosurg* 1997;**23**:47-142.

Gonzalez RG, Schaefer PW, Buonanno FS, *et al.* Diffusion-weighted MR imaging: diagnostic accuracy in patients imaged within 6 hours of stroke symptom onset. *Radiology* 1999;**210**:155-162.

Groenendaal F, Mishra OP, McGowan JE, Hoffman DJ, M Delivoria Papadopoulos. Function of cell membranes in cerebral cortical tissue of newborn piglets after hypoxia and inhibition of nitric oxide synthase. *Pediatr Res* 1990;**42**:174-179.

Hahn PF, Stark DD, Saini S, Lewis JM, Wittenberg J, Ferrucci JT. Ferrite particles for bowel contrast in MR imaging: design issues and feasibility studies. *Radiology* 1987;**164**:37-41.

Hansen AJ, Olsen CE. Brain extracellular space during spreading depression and ischemia. *Acta Physiol Scand* 1980; **108**:355-365.

Hoehn Berlage M, Norris DG, Kohno K, Mies G, Leibfritz D, Hossmann KA. Evolution of regional changes in apparent diffusion coefficient during focal ischemia of rat brain: the relationship of quantitative diffusion NMR imaging to reduction in cerebral blood flow and metabolic disturbances. *J Cereb Blood Flow Metab* 1995;**15**:1002-1011.

Hossmann KA, Fischer M, Bockhorst K, Hoehn Berlage BM. NMR imaging of the apparent diffusion coefficient (ADC) for the evaluation of metabolic suppression and recovery after prolonged cerebral ischemia. *J Cereb Blood Flow Metab* 1994;**14**:723-731.

Hossmann KA, Hoehn Berlage BM. Diffusion and perfusion MR imaging of cerebral ischemia. *Cerebrovasc Brain Metab Rev* 1995; **7**:187-217.

Huppi PS, Barnes PD. Magnetic resonance techniques in the evaluation of the newborn brain. *Clin Perinatol* 1997;**24**:693-723.

Inch WR, McCredie JA, Geiger C, Boctor Y. Spin-lattice relaxation times for mixtures of water and gelatin or cotton, compared with normal and malignant tissue. *J Natl Cancer Inst* 1974;**53**:689-690.

Kimelberg HK. Current concepts of brain edema. Review of laboratory investigations. *J Neurosurg* 1995;**83**:1051-9.

Klatzo I. Neuropathological aspects of brain edema. *J Neuropathol Exp Neurol* 1967;**26**:1-14.

Klatzo I, Chui E, Fujiwara K, Spatz M. Resolution of vasogenic brain edema. *Adv Neurol* 1980;**28**:359-373.

Kohno K, Hoehn Berlage BM, Mies G, Back T, Hossmann KA. Relationship between diffusion-weighted MR images, cerebral blood flow, and energy state in experimental brain infarction. *Magn Reson Imaging* 1995;**13**:73-80.

Lehmenkuhler A, Sykova E, Svoboda J, Zilles K, Nicholson C. Extracellular space parameters in the rat neocortex and subcortical white matter during postnatal development determined by diffusion analysis. *Neuroscience* 1993;**55**:339-351.

Lorek A, Takei Y, Cady EB, et al. Delayed ("secondary") cerebral energy failure after acute hypoxia-ischemia in the newborn piglet: continuous 48-hour studies by phosphorus magnetic resonance spectroscopy. *Pediatr Res* 1994;**36**:699-706.

Loubinoux I, Volk A, Borredon J, et al. Spreading of vasogenic edema and cytotoxic edema assessed by quantitative diffusion and T_2 magnetic resonance imaging. *Stroke* 1997;**28**:419-426.

Lutz PL. The brain without oxygen: causes of failure and mechanisms for survival. Austin, TX: CRC Press, 1994:19

Mathur de Vre R. Biomedical implications of the relaxation behavior of water related to NMR imaging. *Br J Radiol* 1984;**57**:955-976.

Mayahara H, Fujimoto K, Ando T, Ogawa K. A new one-step method for the cytochemical localization of ouabain-sensitive, potassium-dependent p-nitrophenylphosphatase activity. *Histochemistry* 1980;**67**:125-138.

Mayahara H, Ogawa K. Histochemical localization of Na^+-K^+-ATPase. *Methods Enzymol* 1988;**156**:417-430.

Menzies SA, Betz AL, Hoff JT. Contributions of ions and albumin to the formation and resolution of ischemic brain edema. *J Neurosurg* 1993;**78**:257-266.

Mintorovitch J, Moseley ME, Chileuitt L, Shimizu H, Cohen Y, Weinstein PR. Comparison of diffusion- and T_2-weighted MRI for the early detection of cerebral ischemia and reperfusion in rats. *Magn Reson Med* 1991;**18**:39-50.

Mintorovitch J, Yang GY, Shimizu H, Kucharczyk J, Chan PH, Weinstein PR. Diffusion-weighted magnetic resonance imaging of acute focal cerebral ischemia: comparison of

signal intensity with changes in brain water and Na^+-K^+-ATPase activity. *J Cereb Blood Flow Metab* 1994;**14**:332-336.

Moseley ME, Cohen Y, Mintorovitch J, et al. Early detection of regional cerebral ischemia in cats: comparison of diffusion- and T_2-weighted MRI and spectroscopy. *Magn Reson Med* 1990;**14**:330-346.

Mujsce DJ, Christensen MA, Vannucci RC. Cerebral blood flow and edema in perinatal hypoxic-ischemic brain damage. *Pediatr Res* 1990;**27**:450-453.

Naruse S, Aoki Y, Takei R, Horikawa Y, Ueda S. Effects of atrial natriuretic peptide on ischemic brain edema in rats evaluated by proton magnetic resonance method. *Stroke* 1991;**22**:61-65.

Nehlig A, Pereira de Vasconcelos A. Glucose and ketone body utilization by the brain of neonatal rats. *Prog Neurobiol* 1993;**40**:163-221.

Nelson C, Silverstein FS. Acute disruption of cytochrome oxidase activity in brain in a perinatal rat stroke model. *Pediatr Res* 1994;**36**:12-19.

Ning G, Malisza KL, Del Bigio MR, Bascaramurty S, Kozlowski P, Tuor UI. Magnetic resonance imaging during cerebral hypoxia-ischemia: T_2 increases in 2-week-old but not 4-week-old rats. *Pediatr Res* 1999;**45**:173-179.

Pierce AR, Lo EH, Mandeville JB, Gonzalez RG, Rosen BR, Wolf GL. MRI measurements of water diffusion and cerebral perfusion: their relationship in a rat model of focal cerebral ischemia. *J Cereb Blood Flow Metab* 1997;**17**:183-190.

Sigal R. Magnetic resonance imaging: basis for interpretation. New York: Springer-Verlag, 1988:5-17.

Slivka A, Murphy E, Horrocks L. Cerebral edema after temporary and permanent middle cerebral artery occlusion in the rat. *Stroke* 1995;**26**:1061-1065.

Sofka CM, Semelka RC, Kelekis NL, et al. Magnetic resonance imaging of neuroblastoma using current techniques. *Magn Reson Imaging* 1999;**17**:193-198.

Stanimirovic DB, Ball R, Durkin JP. Glutamate uptake and Na^+-K^+-ATPase activity in rat astrocyte cultures exposed to ischemia. *Acta Neurochir* 1997;**70**:1-3.

Stark DD, Weissleder R, Elizondo G, *et al.* Superparamagnetic iron oxide: clinical application as a contrast agent for MR imaging of the liver. *Radiology* 1988;**168**:297-301.

Stejskal EO, Tanner JE. Spin diffusion measurements: spin echoes in the presence of a time-dependent field gradient. *J Chem Phys* 1965;**42**:288-292.

Tengvar C, Forssen M, Hultstrom D, Olsson Y, Pertoft H, Pettersson A. Measurement of edema in the nervous system. Use of Percoll density gradients for determination of specific gravity in cerebral cortex and white matter under normal conditions and in experimental cytotoxic brain edema. *Acta Neuropathol Berl* 1982;**57**:143-150.

Thulborn KR, Waterton JC, Matthews PM, Radda GK. Oxygenation dependence of the transverse relaxation time of water protons in whole blood at high field. *Biochim Biophys Acta* 1982;**714** :265-270.

Towfighi J, Mauger D, Vannucci RC, Vannucci SJ. Influence of age on the cerebral lesions in an immature rat model of cerebral hypoxia-ischemia: a light microscopic study. *Brain Res* 1997;**100**:149-160.

Tuor UI. Local cerebral blood flow in the newborn rabbit: an autoradiographic study of changes during development. *Pediatr Res* 1991;**29**: 517-253.

Tuor UI, Del Bigio MR, Chumas PD. Brain damage due to cerebral hypoxia/ischemia in the neonate: pathology and pharmacological modification. *Cerebrovasc Brain Metab Rev* 1996;**8**:159-193.

Tuor UI, Kozlowski P, Del Bigio MR, et al. Diffusion- and T_2-weighted increases in magnetic resonance images of immature brain during hypoxia-ischemia: transient reversal post hypoxia. *Exp Neurol* 1998;**150**:321-328.

Tuor UI, Kurpita G, Simone C. Correlation of local changes in cerebral blood flow, capillary density, and cytochrome oxidase during development. *J Comp Neurol* 1994; **342**: 439-448.

van Bruggen N, Roberts TP, Cremer JE. The application of magnetic resonance imaging to the study of experimental cerebral ischemia. *Cerebrovasc Brain Metab Rev* 1994;**6**:180-210.

van der Toorn A, Sykova E, Dijkhuizen RM, et al. Dynamic changes in water ADC, energy metabolism, extracellular space volume, and tortuosity in neonatal rat brain during global ischemia. *Magn Reson Med* 1996;**36**:52-60.

van Lookeren Campagne M, Verheul JB, Nicolay K, Balazs R. Early evolution and recovery from excitotoxic injury in the neonatal rat brain: a study combining magnetic resonance imaging, electrical impedance, and histology. *J Cereb Blood Flow Metab* 1994;**14**:1011-1023.

Verheul HB, Balazs R, Berkelbach van der sprenkel JW, et al. Comparison of diffusion-weighted MRI with changes in cell volume in a rat model of brain injury. *NMR Biomed* 1994;**7**:96-100.

Vorisek I, Sykova E. Ischemia-induced changes in the extracellular space diffusion parameters, K^+, and pH in the developing rat cortex and corpus callosum. *J Cereb Blood Flow Metab* 1997;**17**:191-203.

Walton M, Sirimanne E, Reutelingsperger C, Williams C, Gluckman P, Dragunow M. Annexin V labels apoptotic neurons following hypoxia/ischemia. *Neuroreport* 1997;**8**:3871-3875.

Yang GY, Chen SF, Kinouchi H, Chan PH, Weinstein PR. Edema, cation content, and ATPase activity after middle cerebral artery occlusion in rats. Stoke 1992;**23**:1331-1336.

Zhong J, Petroff OA, Prichard JW, Gore JC. Changes in water diffusion and relaxation properties of rat cerebrum during status epilepticus. *Magn Reson Med* 1993;**30**:241-246.